



Review

# Theoretical Studies on the Direct Propylene Epoxidation Using Gold-Based Catalysts: A Mini-Review

Jingjing Ji<sup>1</sup>, Zheng Lu<sup>2</sup>, Yu Lei<sup>2</sup> and C. Heath Turner<sup>1,\*</sup>

- Department of Chemical and Biological Engineering, The University of Alabama, Tuscaloosa, AL 35487, USA; jji4@crimson.ua.edu
- Department of Chemical and Materials Engineering, The University of Alabama in Huntsville, Huntsville, AL 35899, USA; zl0008@uah.edu (Z.L.); yu.lei@uah.edu (Y.L.)
- \* Correspondence: hturner@eng.ua.edu; Tel.: +1-205-348-1733

Received: 3 September 2018; Accepted: 25 September 2018; Published: 27 September 2018



**Abstract:** Direct propylene epoxidation using Au-based catalysts is an important gas-phase reaction and is clearly a promising route for the future industrial production of propylene oxide (PO). For instance, gold nanoparticles or clusters that consist of a small number of atoms demonstrate unique and even unexpected properties, since the high ratio of surface to bulk atoms can provide new reaction pathways with lower activation barriers. Support materials can have a remarkable effect on Au nanoparticles or clusters due to charge transfer. Moreover, Au (or Au-based alloy, such as Au–Pd) can be loaded on supports to form active interfacial sites (or multiple interfaces). Model studies are needed to help probe the underlying mechanistic aspects and identify key factors controlling the activity and selectivity. The current theoretical/computational progress on this system is reviewed with respect to the molecular- and catalyst-level aspects (e.g., first-principles calculations and kinetic modeling) of propylene epoxidation over Au-based catalysts. This includes an analysis of H<sub>2</sub> and O<sub>2</sub> adsorption, H<sub>2</sub>O<sub>2</sub> (OOH) species formation, epoxidation of propylene into PO, as well as possible byproduct formation. These studies have provided a better understanding of the nature of the active centers and the dominant reaction mechanisms, and thus, could potentially be used to design novel catalysts with improved efficiency.

**Keywords:** propylene epoxidation; gold; computational chemistry; active centers; reaction mechanisms

#### 1. Introduction

Due to the growing environmental issues in chemical synthesis and processing, there has been increasing interest in the development of new processes for minimizing pollution and reducing energy consumption. Heterogeneous catalysis plays a crucial role in this respect, since it is widely used to reduce emissions from automobiles, reduce byproducts, and improve the selectivity of important chemical products in the petrochemical as well as other chemical industries [1–5]. Computational and experimental investigators have been working together to better understand fundamental characteristics of a wide range of catalytic reactions. In this paper, we focus on the selective epoxidation of propylene to yield propylene oxide (PO) using heterogeneous gold-based catalysts. The catalytic activity of gold and gold alloy nanoparticles (a few nm in size) has been ascribed to various mechanisms, involving reactions occurring at neutral gold atoms that differ from bulk gold atoms (due to different degrees of coordination), quantum size effects that change the electronic structures of nanoparticles, or charge modification of gold atoms through the interaction with oxide supports [6–8].

Catalysts 2018, 8, 421 2 of 24

Computational studies have been enormously valuable in describing the structural and electronic character of size-selected gold nanoparticles and determining the catalytic reaction mechanisms for the propylene epoxidation process, and have already yielded important outcomes for the development of catalytic materials. Motivated by these growing computational investigations and the need to incorporate this theoretical knowledge into catalyst design, we review the theoretical studies relevant to direct propylene epoxidation in the gas phase with Au-based catalysts. In the following sections, we provide a brief background of propylene epoxidation, and we then highlight different aspects of the propylene epoxidation process, including  $H_2/O_2$  adsorption,  $H_2O_2$  synthesis, and possible epoxidation mechanisms. Finally, conclusions and perspectives are given, along with current challenges and opportunities in the field.

# 2. Background

Propylene oxide (PO) is a key intermediate in the chemical industry. For instance, PO is mainly used to produce polyether polyols (65%), as well as propene glycol (30%) and propene glycol ethers (4%) (the second and third largest applications, respectively), which are mainly applied to manufacture commercial products such as adhesives, solvents, and foams [9–11]. The annual worldwide production of PO in 2013 amounted to 8.06 million tons and will likely go beyond 9.56 million tons in 2018, and this market is annually growing by ~4–5% [11]. The currently available processes are not optimal, since the chlorohydrin process to produce PO suffers from environmental concerns, and the hydroperoxide process (the halcon process) is challenged by poor economics [9,11]. For instance, in the chlorohydrin process, a large amount of byproduct CaCl<sub>2</sub> (2.2 tons per 1.0 ton of PO) is coproduced, along with toxic chlorinated organic compounds (several hundred grams per ton of PO). One problem of the hydroperoxide process is the production of a coproduct (either styrene or *tert*-butyl alcohol, depending on which variant of the hydroperoxide process is applied) in a fixed amount, leading to a mismatch of market demand between PO and co-products.

Compared to the two methods aforementioned, using hydrogen peroxide  $(H_2O_2)$  as the oxidant allows for a high selectivity (95%) for PO production, and it is more environmentally friendly since water is the only byproduct. The major disadvantage for the commercialization of this process is that hydrogen peroxide and PO have comparable market values on a molar basis, which makes it impossible to run the process profitably at this time. Moreover, it requires multiple reaction steps in the liquid phase for purification, which consumes huge amounts of energy. The in situ production of the hydrogen peroxide is currently under construction by Dow-BASF, to solve the high cost of hydrogen peroxide for propylene epoxidation [12].

Another route toward PO production is the direct propylene ( $C_3H_6$ ) epoxidation using gold/titania catalyst in the presence of a mixture of hydrogen and oxygen. For a long time, coinage metal gold was regarded as a catalytically inert material. This common assumption was dramatically shifted by the discovery of low-temperature CO oxidation with metal oxide supported gold nanoparticles [13]. Approximately 20 years ago, Haruta and co-workers discovered that the direct vapor-phase propylene epoxidation with molecular  $H_2$  and  $O_2$  catalyzed by nano-sized gold deposited on  $TiO_2$  (anatase) was a viable route [14]. The largest advantage of gold-on-titania catalysts is that they are able to epoxidize propylene very selectively (>90%) even under mild conditions (typically 323 K and 1 bar), but the activity is relatively low.

Since that time, considerable efforts have been dedicated to enhancing Au-based catalysts, as well as understanding the reaction features of this novel system. For instance, gold particles which are hemispherical in shape are highly active, while spherical nanoparticles possess fairly weak activity [15]. Estimates of the optimal gold nanoparticle size have reduced from  $2\sim5$  nm in diameter to sizes smaller than 2 nm [11,14,16–18]. Haruta's group initially started working with Au nanoparticles supported on  $TiO_2$ , but they gradually transitioned to mesoporous titanosilicates (Ti-SiO<sub>2</sub>) as the supports [19,20]. Delgass's group has focused on microporous titanosilicate (e.g., TS-1) supports, which demonstrate better results, even with low Au loadings [21,22]. The fact that the PO formation requires the presence

Catalysts 2018, 8, 421 3 of 24

of  $H_2$  and  $O_2$ , and the fact that  $C_3H_6$  can be epoxidized by  $H_2O_2$  over titania, generates the common speculation that a peroxide species formed on gold is involved in the propylene epoxidation reaction. In other words, it is proposed that the active oxygen species, hydrogen peroxide, is readily synthesized on nano-sized Au via  $H_2/O_2$  mixtures, and it subsequently transfers to a neighboring Ti site to epoxidize propylene into PO. During this process, the typically low propylene conversion (<2%) and low hydrogen utilization efficiency (<30%) still need to be improved, despite the fact that the selectivity toward PO is high.

Attempts to improve propylene conversion by raising the reaction temperature inevitably lead to decreasing PO selectivity due to consecutive PO reactions (e.g., isomerization, oligomerization, and oxidative cracking) [17,23–26]. For instance, by elevating the reaction temperature from 90 °C to 160 °C, there is an appreciable increase in  $C_3H_6$  conversion from 2.5 to 9.8% over Au/mesoporous Ti-SiO<sub>2</sub>, while the PO selectivity decreases from 95 to 90%. The decrease in selectivity is likely due to the formation of byproducts (e.g., propanal, acetone, ethanal,  $CO_2$ , dioxane, and acids) generated by secondary reactions [19,27]. The byproduct generation is proposed to be related to the dispersity of Ti sites. For example, PO combustion is significantly suppressed if Ti sites are isolated, as in TS-1 and in mesoporous Ti–SiO<sub>2</sub> [28,29]. It is worth noting that acrolein is another significant byproduct [25]. The allylic hydrogen of propylene is acidic and labile, and easily suffers from the nucleophilic attack of the oxygen radicals bound to Au nanoparticles, since the oxygen species behave as a Brønsted base [10,30–32]. Thus, silver-based catalysts, used for commercial production of ethylene oxide (EO) via ethylene epoxidation, lead to propylene combustion versus epoxidation due to the activation of allylic hydrogen by surface O. On the other hand, investigations with regard to gold catalysts indicate that they may be commercially feasible for propylene oxide production [33].

To date, there have been several reviews about the experimental synthesis of PO in the gas phase, including discussions about the development and improvement of Au-based catalysts, propylene conversion, hydrogen efficiency, and PO selectivity [9,11,16,17,34]. At the same time, many theoretical studies have focused on propylene epoxidation with  $\rm H_2$  and  $\rm O_2$  to assist in understanding various aspects of this catalytic reaction. For instance, first-principles calculations can be employed to investigate the elementary events and underlying mechanisms, but it is usually difficult to make statements about the performance of the catalysts under different reaction conditions. In this respect, kinetic modeling studies are needed to evaluate the catalytic activity and product selectivity at larger time and length scales, particularly with several competing reaction pathways. For instance, first-principles based kinetic Monte Carlo (KMC) models can help unravel the reaction mechanism and catalyst complexities in heterogeneous catalytic systems [35–38]. These computation and simulation studies provide detailed insight on how to screen the size and composition of Au nanoparticles, as well as identify catalytic sites and reaction features for the development of commercially viable catalyst for direct PO production.

# 3. The Adsorption of O2 and H2 on Au

Bulk gold surfaces are usually regarded as poor catalysts, at variance with other transition metal surfaces. However, as compared to Au surfaces, small Au particles are known to be active catalysts for a variety of reactions. The adsorption of molecular  $O_2$  and  $H_2$  on small Au clusters in the gas phase is the first step of the overall propylene epoxidation reaction. Thus, this is a key step, since the adsorption energy ( $E_{ads}$ ) can be used as an indicator of activity, and it is helpful for developing a comprehensive understanding of Au catalysis.

Salisbury and co-workers investigated  $O_2$  adsorption on  $Au_n^-$  clusters (n = 2 to 22). They found that  $Au_n^-$  clusters with even n strongly adsorb  $O_2$  molecules, while  $Au_n^-$  clusters with odd n cannot. Salisbury et al. supposed that the adsorbed oxygen molecule exists in the form of  $O_2^-$  species due to charge transfer from the gold [39].

Okumura et al. and Yoon et al., using density functional theory (DFT), studied the interaction between  $O_2$  and Au clusters [40,41]. They found that the anionic Au atoms in gold clusters interact

Catalysts 2018, 8, 421 4 of 24

strongly with  $O_2$  (-12.1 kcal/mol), in contrast with neutral Au atoms (-3~8 kcal/mol), suggesting that negatively charged Au atoms are the active sites for oxygenation. As an extension, Mills et al. suggested that neutral  $Au_n$  clusters with an odd n adsorb  $O_2$  more strongly in contrast with those with even n [42], which agrees well with the recent findings of Chen's group [43]. At the same time, they mentioned that  $O_2$  does not adsorb on flat Au surfaces, indicating that the interaction between  $O_2$  and an Au surface is weak. While in the DFT studies of Mavrikakis and coworkers, they found that, although molecular  $O_2$  does not adsorb on Au(111), it does bind to a stretched Au(111) surface, as well as to both unstretched and stretched Au(211) surfaces with binding energies of -1.84, -3.46, and -6.0 kcal/mol, respectively, implying that steps and tensile strain facilitate the adsorption of  $O_2$  on Au surfaces [7,44].

There is a general agreement regarding the relationship between the increasing activity of gold nanoparticles and a decrease in particle size (leading to a higher concentration of low coordinated gold atoms), as well as particle morphology [6,45]. For instance, Wang and Gong found that an icosahedral  $Au_{32}$  cluster can dissociate molecular  $O_2$ , but the detailed dissociation pathways and the activation energies are not described [46]. Taketsugu et al. studied  $O_2$  adsorption on small neutral gold clusters ( $Au_3$ – $Au_{12}$ ), and found that  $O_2$  adsorption induced structural transformations in gold clusters [47]. Pacchioni et al. also studied  $O_2$  adsorption and dissociation on neutral, positively, and negatively charged  $Au_n$  clusters varying from 5 to 79 atoms [48,49]. It was found that the charging effect of gold clusters is prominent for very small sizes up to about 20–25 gold atoms, in which negatively charged gold clusters are beneficial for  $O_2$  activation, while positively charged clusters are not. The effect of charge disappears with the increasing gold cluster size, and  $Au_{38}$  seems to be the most reactive. When the cluster size increases beyond about 40 atoms, the effect of size and shape becomes a more significant factor governing the reactivity. The electronic properties beyond  $Au_{79}$  linearly scale to the bulk gold properties, and the catalytic activity thus gradually dies out [50].

Corma's group, using DFT calculations, investigated the adsorption and dissociation of  $O_2$  on extended Au(111) and Au(100) surfaces, isolated Au nanoparticles with different sizes (Au<sub>13</sub> and Au<sub>38</sub>) and shapes, and Au nanoparticles supported on  $TiO_2$  [51]. The adsorption energy of  $O_2$  was found to be correlated with gold particle size, and the particle morphology was proved to be a crucial factor for activating  $O_2$  dissociation. They found a linear relationship between the activation energy of  $O_2$  and the net charge on adsorbed  $O_2$ , indicating that the degree of charge transfer determines the molecular  $O_2$  activation. Moreover, they discovered that most of the sites for  $O_2$  adsorption and dissociation are located at the Au/support interface (when gold particles are loaded on a  $TiO_2$  support). This is in good agreement with other investigations, with regard to the high catalytic activity of gold particles loaded on metal oxide supports such as  $CeO_2$ ,  $TiO_2$ , and  $Fe_2O_3$  [6,52–57], as well as metal carbides [58]. Nevertheless, there is still a debate about whether the supports are involved in the formation of charged (positively or negatively, depending on oxidized or reduced support surfaces) Au sites due to a transfer of electron density, if they are involved in the activation of reactants (e.g.,  $O_2$ ), or if they are limited to merely stabilizing the gold particles [59–61].

The adsorption of  $O_2$  on alloy clusters of gold has also been investigated [62,63]. Joshi et al. analyzed the adsorption of  $O_2$  on  $Au_nM_m$  (m,n=0 to 3; M=Cu, Ag, Pd, Pt, and Na) clusters, in which they demonstrated that the alloy trimers containing only one Au atom are most reactive toward  $O_2$ , while those with two Au atoms are least reactive [63]. The  $O_2$  binding energy (BE) follows the trend: BE ( $MAu_2$ ) < BE ( $M_3$ )  $\leq$  BE ( $M_2Au$ ). A Natural Bond Orbital (NBO) analysis indicated that all of the clusters donate electron density to the adsorbed  $O_2$ . Polynskaya et al. calculated the adsorption energies of  $O_2$  on clusters (following the order:  $Au_{20} < Au_{19}Ag < Ag_{19}Au \approx Ag_{20}$ ), and they found dissociative  $O_2$  adsorption is possible on  $Au_{19}Ag$ ,  $Ag_{19}Au$ , and  $Ag_{20}$  clusters [64]. Recently, Feng et al. compared the adsorption of  $O_2$  on the surfaces of pure Au nanoparticles and Au-Ag bimetallic nanoparticles, and found that  $O_2$  adsorption on the Au-Ag alloy is stronger [65]. Their Bader charge calculations showed that the Au atoms on the surface of Au-Ag alloy nanoparticles are negatively charged (prior to  $O_2$  adsorption), implying that there is electron transfer from Ag to Au. When  $O_2$ 

Catalysts 2018, 8, 421 5 of 24

adsorbs on the pure Au or Au–Ag alloy nanoparticles, the adsorbed  $O_2$  can accept electron charge from both nanoparticles, but the  $O_2$  withdraws more charge from the Au–Ag nanoparticle surface than from the pure Au nanoparticle surface. This suggests that the bimetallic Au–Ag nanoparticles tend to donate more electrons to the adsorbed  $O_2$ , thereby facilitating  $O_2$  activation.

In contrast with relatively weak O2 adsorption on Au, H2 adsorption on Au usually follows a dissociative pathway. Gordon's group investigated the reactions of molecular hydrogen with small gold clusters and showed that molecular H<sub>2</sub> easily binds to neutral Au<sub>2</sub> and Au<sub>3</sub> clusters, and then dissociates into two hydrogen atoms [66]. Through DFT calculations, Barrio et al. studied the interaction between H<sub>2</sub> and Au(111), Au(100), and Au clusters (Au<sub>14</sub>, Au<sub>25</sub>, and Au<sub>29</sub>). They found that the H-H bond was spontaneously elongated up to cleavage, without an apparent activation barrier, when H<sub>2</sub> approached the Au clusters. H<sub>2</sub> dissociation was also found to be accompanied by the deformation of clusters in order to stabilize the dissociated H atoms. This is different from H<sub>2</sub> dissociation on the more rigid icosahedral Au<sub>13</sub> cluster, with an activation energy of 6.93 kcal/mol [67]. Recently, studies of H<sub>2</sub> adsorption and dissociation on gold clusters demonstrated not only that the effect of low coordinated Au atoms is important, but also that the fluxionality (the flexibility of the structure) and ensemble effects play key roles in the bonding and dissociation of H<sub>2</sub> [68]. Simultaneously, Barrio et al. found that the flat (111) and (100) surfaces of bulk gold are not active towards H<sub>2</sub> dissociation [69,70], which is in agreement with previous studies [71]. Flores et al. also obtained a similar conclusion that stretched gold nanowires are more catalytically active for H<sub>2</sub> dissociation in comparison to the Au(111) surface (H<sub>2</sub> dissociation barriers: 9.22 vs. 23.06 kcal/mol) [72].

In addition to Au surfaces and nanoparticles,  $H_2$  dissociation at the perimeter sites of  $Au/TiO_2$  has been explored by several groups. For instance,  $H_2$  et al. investigated the dissociation of molecular  $H_2$  at an  $Au/TiO_2$  interface, as well as atomic  $H_2$  spillover from Au nanoparticles to a  $TiO_2$  support [73]. In their studies,  $H_2$  dissociation is possible via two different modes, namely homolytic and heterolytic routes. In the homolytic pathway,  $H_2$  dissociates on the Au atoms only, while in the heterolytic one,  $H_2$  dissociation occurs on one Au atom and a nearby surface O (from  $TiO_2$ ). It was found that the heterolytic dissociation of molecular  $H_2$  is more favored than the homolytic dissociation (with activation barriers of 8.53 vs. 14.76 kcal/mol) at the perimeter sites of  $Au/TiO_2$ . Using DFT calculations, Takeda's group verified the transition state structure  $O^2-H^+-H^--Au$  of  $H_2$  dissociation at the perimeter of  $TiO_2$ , as  $H\ddot{u}$ ckel's theory initially suggested [74]. Simultaneously, they demonstrated that  $H_2$  dissociation at the perimeter sites has the lowest activation barrier (6.23 kcal/mol) in contrast with those on Au(100), Au(321), and the  $TiO_2$  support (17.53, 14.76, and 18.68 kcal/mol, respectively). The calculated activation barrier of 6.23 kcal/mol is consistent with the theoretical result (6.69 kcal/mol) from Hu's group aforementioned but is higher than the reported 3.69 kcal/mol from Neurock's group [75]. Their results are lower than the experimental estimate of 8.76 kcal/mol [76].

# 4. The Synthesis of H<sub>2</sub>O<sub>2</sub> from O<sub>2</sub> and H<sub>2</sub>

Hydrogen peroxide ( $H_2O_2$ ) is a green oxidant, and it has been listed as one of the 100 most important chemicals in the world [77]. The annual worldwide production of  $H_2O_2$  in 2010 was about 3 million tons [78], in which the auto-oxidation (AO) method accounts for more than 95% of the synthesis. However, the AO process is accompanied by problems of exhaust gas emission, solid waste, and waste water [77]. Currently, most commercial  $H_2O_2$  production is directed towards applications in wastewater treatment, hydroquinone production, bleaching of textile and pulp, removal of organic pollutants, etc. [79–81]. In recent years, commercial  $H_2O_2$  has been used in chemical synthesis, such as the epoxidation of alkenes [82]. Unlike the AO process, the direct synthesis of  $H_2O_2$  with  $H_2$  and  $O_2$  emerges as an atomically economic and green chemical reaction, catalyzed by noble metals, such as Pd, Pt, Au, and Ru. Since this review focuses on propylene epoxidation with Au-based catalysts, we highlight the relevant theoretical studies of  $H_2O_2$  production from  $H_2$  and  $O_2$  involving gold catalysts.

Catalysts 2018, 8, 421 6 of 24

Thomson's group proposed a reaction path for H<sub>2</sub>O<sub>2</sub> formation on a neutral Au<sub>3</sub> cluster as shown in Figure 1 [83]. The first step is nondissociative O<sub>2</sub> adsorption on an Au trimer with an end-on gentimet 2018-86-ktcalt/litible literality energy). As molecular H<sub>2</sub> approaches the adsorbed O<sub>2</sub>, the H-Hobords gradually elongates to breakage and one H directly bonds to one Au atom, and the other H bonds to an hetweed to concret. An atom another musers and a the fry dropper the scounce 1991th Inscinate wear formation Antermediated in Figure 1 of the Isoarrated XF Pader Cost of lewing by the exothermic addition at the elecutar (Pe. 19. Interpretated interpretation), are higher seen by structural rearrangement to respectate by terrordiate Acallevians this cataly turical see a peat. The Alexagorien has the bishast antivationatearian (AFig this catalight) movine turiose the Thorngoigue of this forest the regident discounting Baspezaket al bayredephonetenten that small areutral bold obest per locate. Aurkand sa una cap zakaly ar. HAVE dermation can have adentified possible steaction, pathways Aug both Etaly and Holosynthesis, and never definitive the second process of the process of the second process of the seco bighlight anymartant fluctuations are the male cluster charings the more simulations shighlights impossion to mith the sepmetric Auxinoality of Aux norticles after process, which is a territory on the compared thex cotal Nti Coracivity reference and continuous continuous control of the continuous control of the continuous control of the control of t formu H2Q1 18 Au It awas Agund that both he entral hand charged of victority of social files of the social social formula and social files of the formation reaction duct and that because tarives one for the interpetion de sen anthe federal second second se  $\mathbb{R}^{f}$  the inotinative one for  $H_2O_2$  formation based on the Gibbs free energy of activation.

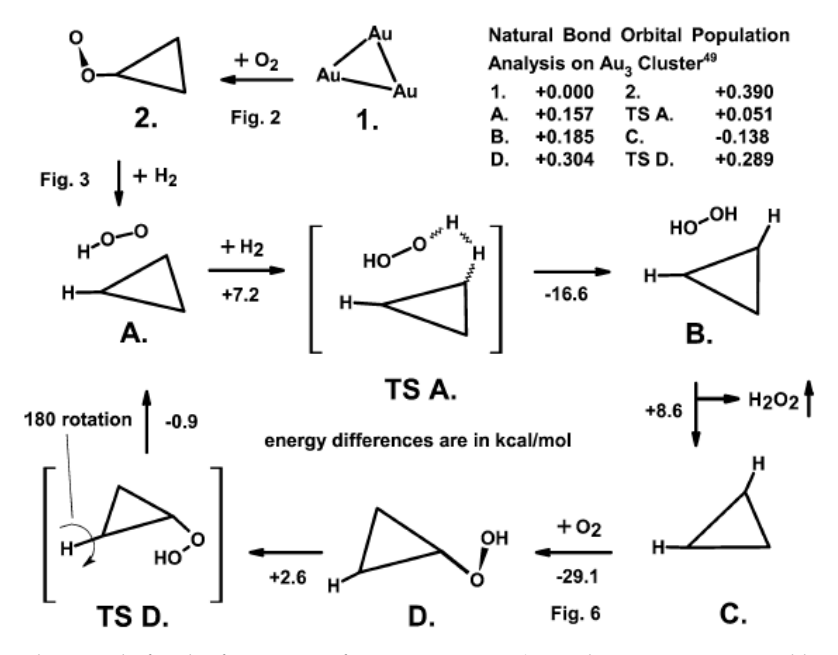


Figure 1. Catalytic cycle for the formation of H<sub>2</sub>O<sub>2</sub> over Au<sub>3</sub> (Au<sub>3</sub> cluster is represented by the triangle figure 1. Catalytic cycle for the formation of H<sub>2</sub>O<sub>2</sub> over Au<sub>3</sub> (Au<sub>3</sub> cluster is represented by the triangle in each intermediate geometry) with two transition state geometries (TS A and TS D), identified with square brackets, and intermediates (A-D). Energy differences are shown in kcal/mol under each square brackets, and intermediates (A-D). Energy differences are shown in kcal/mol under each reaction arrow [83]. Copyright © 2004 Elsevier Inc.

As mentioned above, the adsorption of O<sub>2</sub> on Au particles is weak. However, it has been shown As mentioned above the adsorption of O<sub>2</sub> on Au particles is weak. However, it has been shown that the reactivity of Au(111) and Au(100) surfaces and clusters toward O<sub>2</sub> is noticeably enhanced that the presence of preadsorbed hydrogen. In this case, the interaction between Au and O<sub>2</sub> becomes with the presence of preadsorbed hydrogen. In this case, the interaction between Au and O<sub>2</sub> becomes with the presence of preadsorbed hydrogen. In this case, the interaction between Au and O<sub>2</sub> becomes with the presence of preadsorbed hydrogen. In this case, the interaction between Au and O<sub>2</sub> becomes with the presence of preadsorbed hydrogen. In this case, the interaction between Au and O<sub>2</sub> becomes with the presence of preadsorbed hydrogen. In this case, the interaction between Au and O<sub>2</sub> becomes with the presence of preadsorbed hydrogen. In this case, the interaction between Au and O<sub>2</sub> becomes with the presence of the formation of O-H bonds, leading to easier formation of the active oxidant species stronger due to the formation of O-H bonds, leading to easier formation of the active oxidant species complete the properties of the

Catalysts 2018, 8, 421 7 of 24

peroxide (HOOHH), hydroxyl (OH), and water ( $H_2O$ ). It is clearly seen that the elementary reactions concerning O–O bond breakage (e.g., O–O, O–OH, HO–OH, and O–OHH) directly or indirectly bring about  $H_2O$  formation. The results demonstrate that (1) the dissociative adsorption of  $O_2$  prevails on Rh, Ir, Ni, and Cu facets, and the reduction of the dissociated O species is kinetically hindered due to the strong O binding to the metals; (2) the complete reduction to  $H_2O$  via species OOH, HOOH, and OOHH prevails on Pd, Pt, and Ag, since they are capable of catalyzing O–O bond cleavage and O–H bond formation; (3) Au cannot easily break the O–O bond due to the weak binding of  $O_2$ . Therefore, Au is more selective towards the partial reduction of  $O_2$  to generate  $H_2O_2$ .

#### Adsorption

$$O_2(g) \rightarrow O_2$$
 (1)

## Hydrogenation

$$O_2 + H \rightarrow OOH$$
 (2)

$$OOH + H \rightarrow HOOH \tag{3}$$

$$OOH + H \rightarrow OOHH \tag{4}$$

$$HOOH + H \rightarrow HOOHH$$
 (5)

$$O + H \rightarrow OH$$
 (6)

$$OH + H \rightarrow H_2O \tag{7}$$

$$2OH \rightarrow H_2O + O \tag{8}$$

#### O-O bond scission

$$O_2 \rightarrow 2O$$
 (9)

$$OOH \rightarrow OH + O \tag{10}$$

$$HOOH \rightarrow 2OH$$
 (11)

$$OOHH \rightarrow H_2O + O \tag{12}$$

## Desorption

$$HOOH \rightarrow HOOH (g)$$
 (13)

$$H_2O \rightarrow H_2O(g)$$
 (14)

Since Hutchings and coworkers discovered the synergistic effect of bimetallic PdAu on the direct synthesis H<sub>2</sub>O<sub>2</sub> in 2002 [87], several analyses of H<sub>2</sub>O<sub>2</sub> formation from H<sub>2</sub> and O<sub>2</sub> on alloy clusters have been reported. Through first principles calculations, Thomson's group predicted the catalytic activity of Ag-Au, Cu-Au, and Pd-Au dimers and trimers for H<sub>2</sub>O<sub>2</sub> formation, including several elementary steps: (1) molecular adsorption of O<sub>2</sub>, (2) the formation of OOH species due to the first H addition, and (3) the formation of H<sub>2</sub>O<sub>2</sub> based on the second H addition [88]. For each step, the activation energy ( $\Delta E_{act}$ ) and the change in the Gibbs free energy ( $\Delta G_{act}$ ) were computed. It was shown that the H<sub>2</sub>O<sub>2</sub> formation on small Ag–Au and Cu–Au clusters is not feasible, mainly because of the unfavorable thermodynamics of H<sub>2</sub> addition. On the other hand, the formation of the OOH and H<sub>2</sub>O<sub>2</sub> species is both thermodynamically and kinetically favorable on the PdAu dimer, while it is thermodynamically unfavorable on PdAu<sub>2</sub> and Pd<sub>2</sub>Au trimers. Consequently, the PdAu dimer is proposed as a potentially active cluster for both OOH and H<sub>2</sub>O<sub>2</sub> formation (in contrast with other clusters), implying that H<sub>2</sub>O<sub>2</sub> formation is very sensitive to the size as well as the composition of the alloying clusters. This result is consistent with Ham's studies [89,90], in which they demonstrated that the surface reactivity of bimetallic alloys is mostly influenced by the creation of unique mixed-metal surface sites (the so-called ensemble (geometry) effect [91]). Three different Pd monomer systems in the slab and cluster geometries involving AuPd<sub>M</sub>/Pd(111), AuPd<sub>M</sub>/Au(111)

Catalysts 2018, 8, 421 8 of 24

(M represents a Pd monomer), and  $Au_{41}Pd@Pd_{13}$  are used to examine how surface electronic structure impacts the ensemble effect for  $H_2O_2$  formation. In contrast with  $Au_{41}Pd@Pd_{13}$  and  $AuPd_M/Au(111)$  cases,  $AuPd_M/Pd(111)$  has a higher  $H_2O_2$  selectivity. The  $AuPd_M/Pd(111)$  shows lower activation barriers for OOH and  $H_2O_2$  formation (12.22 and 8.53 kcal/mol, respectively) compared to that on  $Au_{41}Pd@Pd_{13}$  (16.60 and 14.30 kcal/mol, respectively) and  $AuPd_M/Au(111)$  (11.76 and 16.37 kcal/mol, respectively). However, the activation barriers for OOH and  $H_2O_2$  decomposition are higher (18.68 and 7.15 kcal/mol, respectively), as compared to that on  $Au_{41}Pd@Pd_{13}$  (10.38 and 3.92 kcal/mol, respectively) and  $AuPd_M/Au(111)$  (7.38 and 5.30 kcal/mol, respectively). The reactivity enhancement of the Pd and Au surface atoms is a consequence of the reduced coordination number, as well as the inherent mechanical strain. As a result, the enhanced activity of Pd and its adjacent Au atoms makes the bond breakage of O–O, O–OH, and HO–OH easier, leading to decreased  $H_2O_2$  selectivity. In the formation of  $H_2O_2$  on  $Au_{20}$  and  $Au_{19}Pd$  clusters, Beletskaya et al. also concluded that the substitution of gold atoms by palladium in  $Au_{20}$  results in an increase in the activity of catalyst for  $H_2O_2$  formation, while low coordinated palladium atoms are also responsible for decreasing the selectivity due to water formation [92].

Yoshizawa et al. examined the formation of H<sub>2</sub>O<sub>2</sub> from H<sub>2</sub> and O<sub>2</sub> on Pd(111) and Au@Pd(111) and 10 possible elementary steps were considered [93-95]. All of the side reactions are involved in O–O bond cleavage (e.g., O–O, O–OH, and HO–OH), leading to the nonselective formation of H<sub>2</sub>O. It is proposed that the competition of  $H_2O_2$  and  $H_2O$  formation is actually the competition between the O-O bond and O-M bond (M is Pd in the case of the Pd(111) and Au in the case of the Au@Pd(111)). The O-Pd bond is usually stronger than the O-O bonds in the OOH and H<sub>2</sub>O<sub>2</sub> species, making the O-O bond breakage facile, while the O-Au bond is generally weaker than the O-O bonds, suppressing the O-O bond dissociation and thus facilitating the release of H<sub>2</sub>O<sub>2</sub>. Similar conclusions are also obtained in Todorovic's findings [96], in which they demonstrate that the H<sub>2</sub>O formation mainly originates from O<sub>2</sub> dissociation on Pd(111), while it is formed from H<sub>2</sub>O<sub>2</sub> decomposition on Au(111). One intuitive explanation is that each additional H atom weakens the bond of the molecular backbone and increases the O–O bond length. Nørskov et al. have shown that the O–O bond length increases as  $O_2$  (1.34 Å), OOH (1.44 Å), and  $H_2O_2$  (1.50 Å) on an  $Au_{12}$  cluster [97]. Moreover, using well-established scaling and Brønsted-Evans-Polanyi (BEP) relations in combination with the concept of the degree of catalyst control, they predict a search direction for promising H<sub>2</sub>O<sub>2</sub> synthesis catalysts, where binary Au–Pd and Au-Ag alloys are most promising (taking stability considerations into account).

#### 5. PO Reaction Mechanism

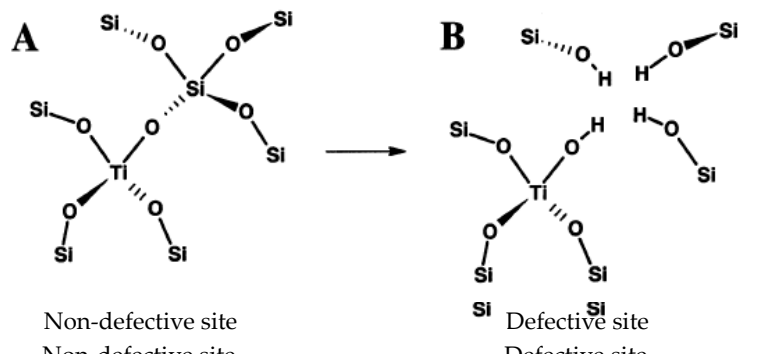
Haruta and co-workers first demonstrated the direct propylene epoxidation using gas-phase  $H_2$  and  $O_2$  over  $Au/TiO_2$  with high selectivity [14]. Since then, Au nanoparticles supported on several other Ti-containing supports (such as TS-1 [10,29], Ti-MCM-41 [98], and Ti-MCM-48 [26]) have been found to be active for propylene epoxidation in the gas phase. In particular, Au nanoparticles loaded on a TS-1 support were first synthesized at Enichem (Italy) [99] and were identified as a possible candidate for the future commercial production of PO. Because of the adequate activity, high selectivity, and extraordinary stability of TS-1, liquid-phase epoxidation using  $H_2O_2$  over TS-1 is feasible for PO production [100,101]. However, in view of the fact that  $H_2O_2$  and PO have comparable market values on a molar basis, currently, it is difficult to run this process profitably. An inelastic neutron scattering (INS) study [102] and in situ UV spectroscopy study [103] have offered direct spectroscopic evidence for the formation of  $H_2O_2$  and the hydroperoxy radical (OOH) species, originating from  $H_2-O_2$  related reactions over  $Au/TiO_2$ . Thus, a similar propylene epoxidation mechanism in the gas phase using in situ formed  $H_2O_2$  over Au/TS-1 catalyst is expected.

In many cases, current theoretical studies are on par with classical experimental analyses, so theory and experiment can drive each other towards a better understanding of the catalytic reaction mechanism of propylene epoxidation and catalyst design. In the following sections, we summarize the application of computational catalysis and kinetic modeling for the propylene epoxidation mechanism

Catalysts 2018, 8, 421 9 of 24

Catalysts **2018**, 8, x FOR PEER REVIEW (as well as possible side reactions), involving (1) epoxidation using  $H_2O_2$  over TS-1; (2)  $H_2O_2$  formation Catalysts **2018**, 8, x FOR PEER REVIEW 9 of 23 and propylene epoxidation and Au; and (3) the synergistic effect of an Au/Ti-containing support. S.1. Reaction Mechanism on Titanosilicate

5.1. Reaction Mechanism on Titanosilicate catalitic ampletisor and the particles supported on titanosilicate (TS-1) present much higher catalitic amplication to Author 2014 particles supported on titanosilicate (TS-1) present much higher catalitic activity for the author of the particles supported on titanosilicate (TS-1) present much higher the Titisites is in the first propriet of the author of the auth



Non-defective site

Figure 2. Schematic view of (A) a fully tetrahedral Ti site bonded with four O–Si groups, and (B) the

Figure 2. Schematic view of (A) a fully tetrahedral Ti site bonded with four O–Si groups, and (B) the

Figure 2. Schematic view of (A) a fully tetrahedral Ti site bonded with four O–Si groups, and (B) the

Figure 2. Schematic view of (A) a fully tetrahedral Ti site bonded with four O–Si groups, and (B) the

Figure 2. Schematic view of (A) a fully tetrahedral Ti site bonded with four O–Si groups, and (B) the

Figure 2. Schematic view of (A) a fully tetrahedral Ti site bonded with four O–Si groups, and (B) the

Figure 2. Schematic view of (A) a fully tetrahedral Ti site bonded with four O–Si groups, and (B) the

Figure 2. Schematic view of (A) a fully tetrahedral Ti site bonded with four O–Si groups, and (B) the

Figure 2. Schematic view of (A) a fully tetrahedral Ti site bonded with four O–Si groups, and (B) the

Figure 2. Schematic view of (A) a fully tetrahedral Ti site bonded with four O–Si groups, and (B) the

Figure 2. Schematic view of (A) a fully tetrahedral Ti site bonded with four O–Si groups, and (B) the

Figure 2. Schematic view of (A) a fully tetrahedral Ti site bonded with four O–Si groups, and (B) the

Figure 2. Schematic view of (A) a fully tetrahedral Ti site bonded with four O–Si groups, and (B) the

Figure 2. Schematic view of (A) a fully tetrahedral Ti site bonded with four O–Si groups, and (B) the

Figure 2. Schematic view of (A) a fully tetrahedral Ti site bonded with four O–Si groups, and (B) the

Figure 2. Schematic view of (A) a fully tetrahedral Ti site bonded with four O–Si groups, and (B) the

Figure 2. Schematic view of (A) a fully tetrahedral Ti site bonded with four O–Si groups, and (B) the

Figure 2. Schematic view of (A) a fully tetrahedral Ti site bonded with four O–Si groups, and (B) the

Figure 2. Schematic view of (A) a fully tetrahedral Ti site bonded with fully tetrahedral Ti site bonded with fully tetrahedral Ti site bonded with fully tetrahedral Ti sit

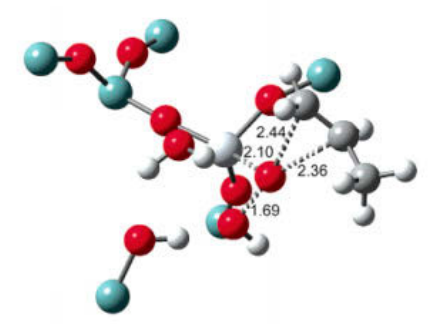
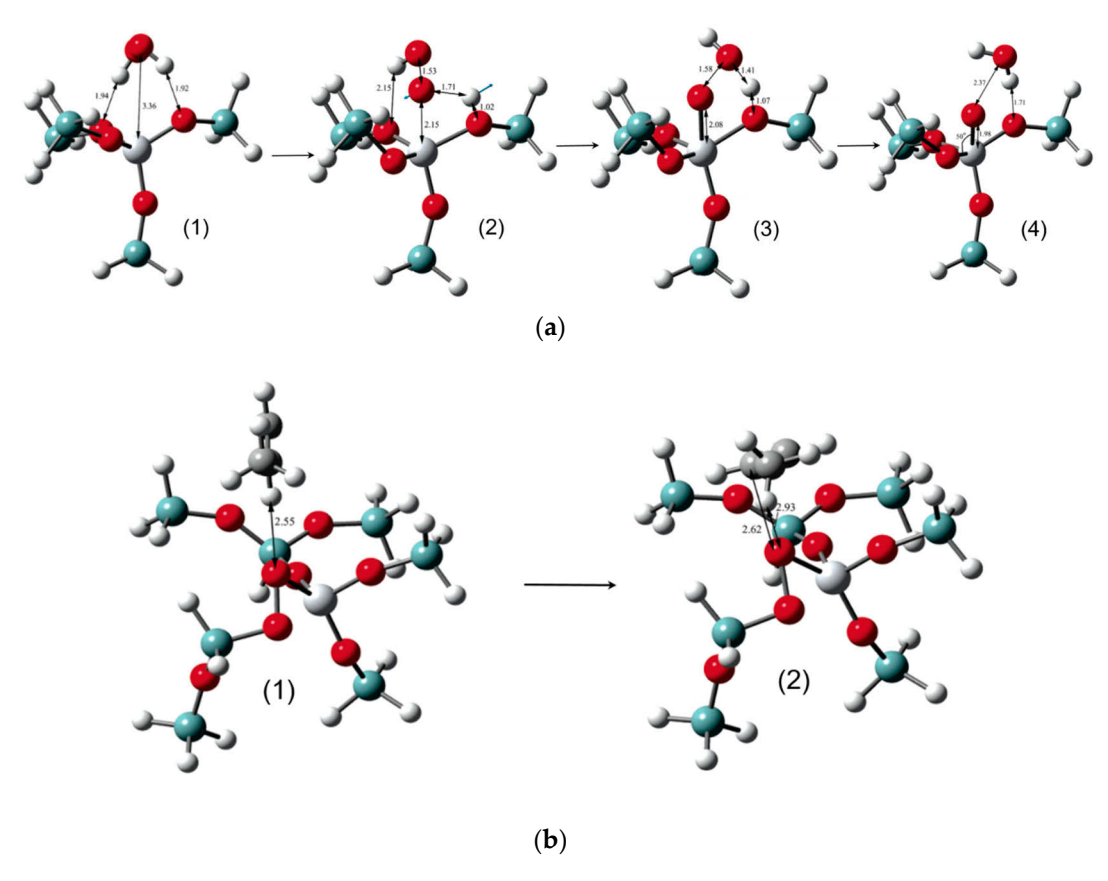


Figure 3. Transition state for the reaction of the hydroperoxy intermediate on a defect Ti site with Figure 3. Transition state for the reaction of the hydroperoxy intermediate on a defect Ti site with Figure 3. Transition state for the reaction of the hydroperoxy intermediate and defect Ti site with Figure 3. Transition state for the reaction of the hydroperoxy intermediate and defect Ti site with Figure 3. The properties of the hydroperoxy intermediate on a defect Ti site with Figure 3. The properties of the hydroperoxy intermediate on a defect Ti site with Figure 3. The properties of the hydroperoxy intermediate on a defect Ti site with Figure 3. The properties of the hydroperoxy intermediate on a defect Ti site with Figure 3. The properties of the hydroperoxy intermediate on a defect Ti site with Figure 3. The properties of the hydroperoxy intermediate on a defect Ti site with Figure 3. The properties of the hydroperoxy intermediate on a defect Ti site with Figure 3. The properties of the hydroperoxy intermediate on a defect Ti site with Figure 3. The properties of the hydroperoxy intermediate on a defect Ti site with Figure 3. The properties of the hydroperoxy intermediate on a defect Ti site with Figure 3. The properties of the hydroperoxy intermediate on a defect Ti site with Figure 3. The properties of the hydroperoxy intermediate on a defect Ti site with Figure 3. The properties of the hydroperoxy intermediate on a defect Ti site with Figure 3. The properties of the hydroperoxy intermediate on a defect Ti site with Figure 3. The properties of the hydroperoxy intermediate on a defect Ti site with Figure 3. The properties of the hydroperoxy intermediate on a defect Ti site with Figure 3. The properties of the hydroperoxy intermediate on a defect Ti site with Figure 3. The properties of the hydroperoxy intermediate on a defect Ti site with Figure 3. The properties of the hydroperoxy in the hyd

Inntheinal discriptions in the property of the property of the possible mechanisms for property epoxiliation in slate H2004 ites. The characteristic compared first property of the property o

oxygen from the Si–O–O–Ti species then inserts into the C=C double bond of the adsorbed propylene molecule ( $\Delta E_{act} = 1.2 \text{ kcal/mol}$ ), as shown in Figure 4b.

The last two mechanisms involve defect sites, based on a partial silanol nest model and a full silanol nest model, respectively. As Figure 2 shows, a Ti site with one defect neighbor means a total Catalysts 2018, 8, 421 of three neighboring hydroxyl groups (or silanol groups, Si–OH). In the partial silanol nest model, only one Si–OH group is modeled instead of three, and the epoxidation mechanism mentioned above is studied with [the ]transition statepseausothed here, and the epoxidation mechanism mentioned above is studied with [the ]transition statepseausothed here, and the epoxidation mechanism mentioned above is studied with [the ]transition statepseausothed here. and the epoxidation mechanism mentioned above is studied with [the ]transition statepseausothed here. It is the proposed for the partial siland here. The proposed for the expectation of the partial siland here. The proposed for the partial siland here. The partial siland here. The partial siland here. The proposed for the partial siland here. The partial siland h

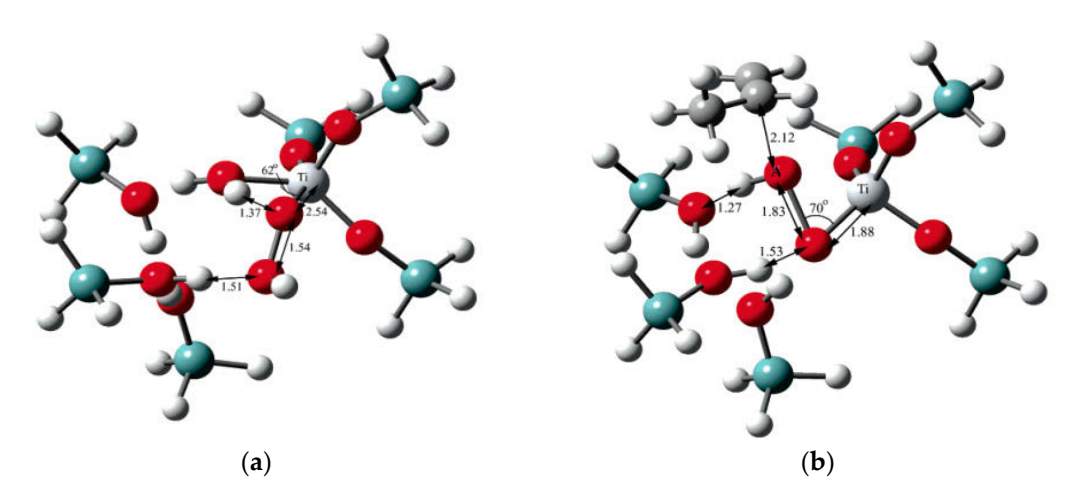


Higure 4. Munadataet all mechanism (a)a) the formation of Sicocott is pecies, where (1) is the preadsorbed complex of H202001TS41 (2) is the transition state geometry for the first step in oxygen insertion to the peroxo intermediate on the dosed Tisite (3) is the stable intermediate geometry prior to the second step tep by geny perior to the peroxo intermediate on the dosed Tisite (3) is the stable intermediate geometry prior to the second step tep by geny perior to the second step tep by geny period to the period step is conferred in passion to the period step is conferred in properties and step is conferred to period step is conferred to the period step in the period step in the period step of the period step in the period

The last two mechanisms involve defect sites, based on a partial silanol nest model and a full silanol nest model, respectively. As Figure 2 shows, a Ti site with one defect neighbor means a total of three neighboring hydroxyl groups (or silanol groups, Si–OH). In the partial silanol nest model, only one Si–OH group is modeled instead of three, and the epoxidation mechanism mentioned above is studied, with the transition-state geometry shown in Figure 3 [32]. In the full silanol nest model, the formation of a hydroperoxy intermediate (Ti–OOH) overcomes an activation barrier of 8.9 kcal/mol (Gibbs free energy at 298 K), with the transition-state structure shown in Figure 5a. Once the generated H<sub>2</sub>O is removed from the active site, propylene can adsorb and react with the active Ti–OOH species. The activation energy for the transition-state structure (Figure 5b) is only 4.6 kcal/mol (Gibbs free energy at 298 K). In comparison to a partial silanol nest model, the Ti/defect site pathway with a full

Catalysts 2018, 8, 421 11 of 24

silanol nest is energetically more favorable with regard to the propylene epoxidation in the  $H_2O_2/TS-1$  Catalys  $H_2O_1$  AFO (TISHREMEN): systems.



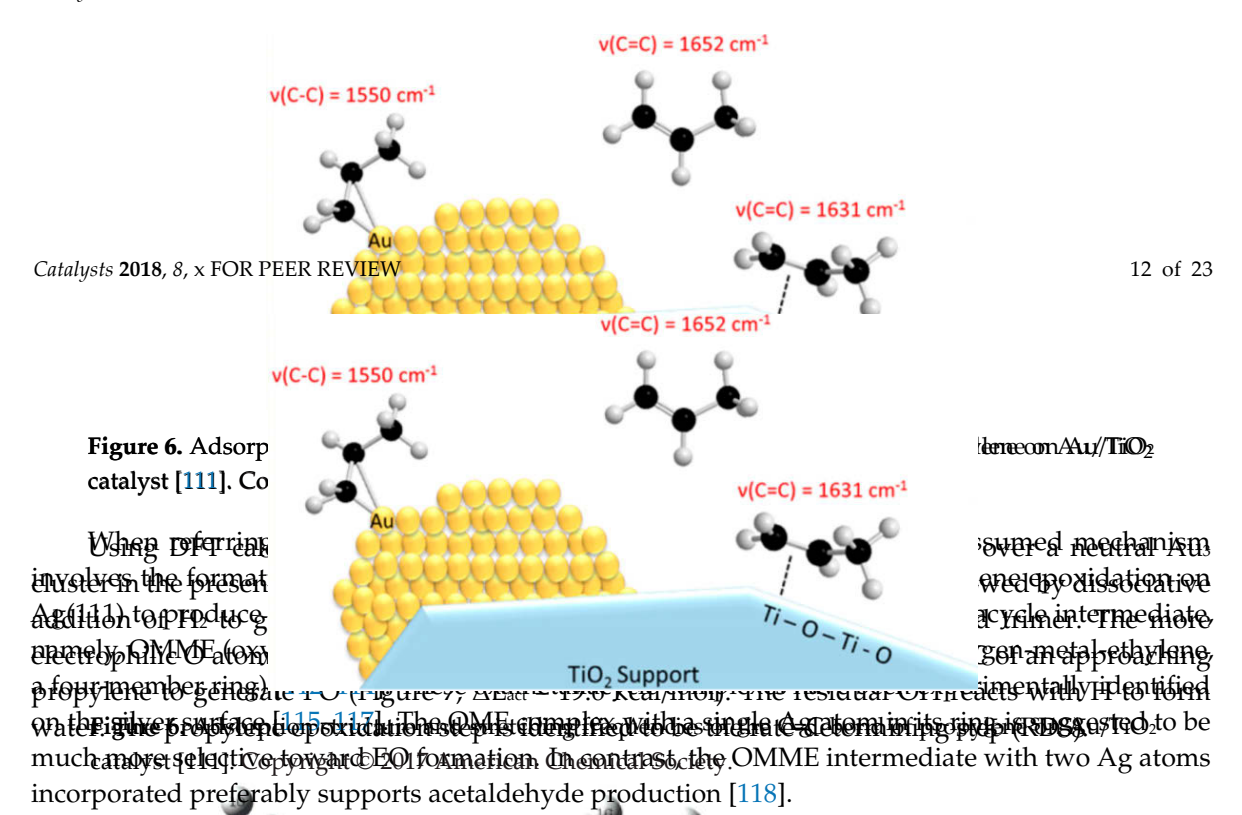
FigFigure Ti/diffedefact chardsonism for the Helfull side of the System (a) transition to the Helfull side of TS-11, and (b) transition-state geometry for for propply the possibilities of 1914 Pitatorical substances shower in a white of the property of 2016 a remission of the Property of 2016 are the substances of the Property of th

Referry, to Songress and personal of Tarahalations to insurgive the proposition personal attention memorianism with the Overent triangle hard. The defect of the first and all and the Overent triangle hard. The defect of the first and all and the defect represent the proposes of the first of the first and the sites of the first and the first and the sites of the first and the first and the personal of the first and the consense of the first and the first and the consense of the first and the first and the consense of the first and the first and the consense of the first and the first and the consense of the first and th

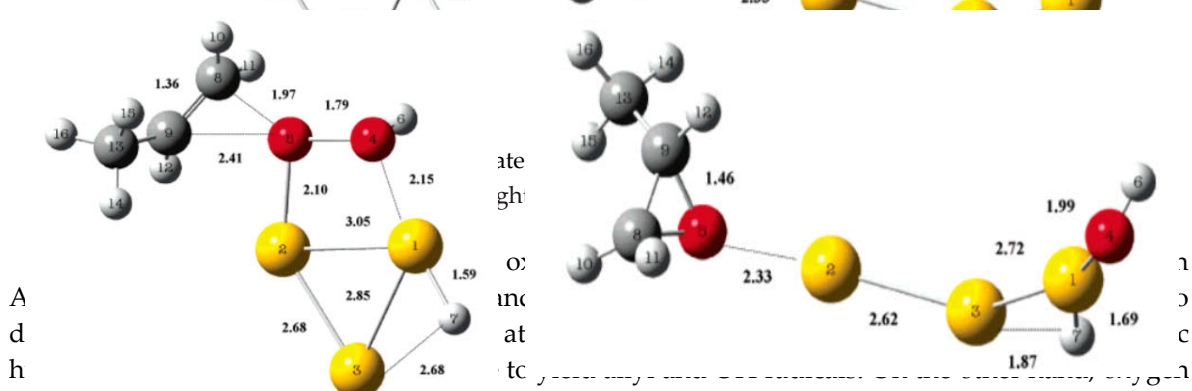
# 5.2. Reaction Mechanism on Gold 5.2. Reaction Mechanism on Gold

In addition to the aforementioned reaction mechanisms on TS-1 in which propylene attacks active Ti—OOH (or Ti—H<sub>2</sub>O<sub>2</sub>) species, recent DFT studies in combination with Fourier transform infrared active Ti—OOH (or Ti—H<sub>2</sub>O<sub>2</sub>) species, recent DFT studies in combination with Fourier transform infrared (FTIR) spectroscopy have identified the adsorption of propylene and PO on the Au/TiO<sub>2</sub> catalyst interface [110 Ti11]. Propylene was found to bind to a single atomic Au atom site via a (πο)-interaction and bind to the TiO<sub>2</sub> surface via a π-interaction, and this interaction is also distinguishable through the C=C bond stretching frequency of propylene (Tipure 6). The results reveal that the propylene—Au (particularly low coordinated Au atoms, e.g. corner and edge sites) interaction has a stronger binding stronger binding energy in comparison to the propylene—TiO<sub>2</sub> interaction, suggesting a possible epoxidation for the propylene of the propylene—TiO<sub>2</sub> interaction, suggesting a possible epoxidation for the propylene of the propylene—TiO<sub>2</sub> interaction, suggesting a possible epoxidation for the propylene of the propylene—TiO<sub>2</sub> interaction, suggesting a possible epoxidation for the propylene of the propylene—TiO<sub>2</sub> interaction, suggesting a possible epoxidation for the propylene of the propylene—TiO<sub>2</sub> interaction, suggesting a possible epoxidation for the propylene of the propylene—TiO<sub>2</sub> interaction, suggesting a possible epoxidation for the propylene of the propylene—TiO<sub>2</sub> interaction, suggesting a possible epoxidation for the propylene of the propylene—TiO<sub>2</sub> interaction, suggesting a possible epoxidation for the propylene of the propylene of the adsorption of propylene on an Au(111) propylene of the adsorption strength was found to follow the trend: defect free the vacancy of the propylene of the adsorption strength was found to follow the trend: defect free the vacancy of the propylene addatom (a) indicating that the low, coordinated Au sites et years the propylene addatom can activate propylene to some exten

When referring to the olefin epoxidation process, the most commonly assumed mechanism involves the formation of an oxametallacycle intermediate. For example, ethylene epoxidation on Ag(111) to produce ethylene oxide (EO) is considered to undergo an oxametallacycle intermediate, namely, OMME (oxygen-metal-ethylene, a five-member ring) or OME (oxygen-metal-ethylene, a four-member ring) [112–114]. These oxametallacycle complexes have been experimentally identified on the silver surface [115–117]. The OME complex with a single Ag atom in its ring is suggested to be much more selective toward EO formation. In contrast, the OMME intermediate with two Ag atoms incorporated preferably supports acetaldehyde production [118].



Using DFT calculations, Thomson et all. explored propylene epoxidation over a mentral  $Au_3$  cluster in the presence of  $H_2$  and  $O_2$  [119]. A side-on  $O_2$  adsorption on  $Au_3$  is followed by dissociative addition of  $H_2$  to generate an OOH species and a long  $H_3$  located on the gold trimer. The more electrophilic  $O_3$  atom (proximal to the  $Au_3$ ) of the  $Au_4$ -OOH group attacks the C=C of an approaching propylene to generate  $PO_3$  ( $H_3$ ) where  $H_3$  is identified to real material of  $H_3$  reacts with  $H_4$  to form water. The propylene epoxidation step is identified to real protection and  $H_3$  is followed by dissociative addition of  $H_3$  and  $H_4$  is form water. The propylene epoxidation of  $H_4$  is identified to real propylene epoxidation of  $H_4$  is identified to real propylene epoxidation of  $H_4$  is identified to real propylene epoxidation of  $H_4$ .



works as a Lewis acid, receiving electronic density from the C=C bond of propylene to lead to the form Figure & Structure of the dynamic final particle dupting the apprehensive on Austrice members are in presented with A Copyright 19200 Austrice Chromol Switch 11 in which atomic O is bound to the end C of the C=C and the middle C of propylene is linked to the Au surface, or OMMP2 in which et al. in the structure of the middle C of propylene is linked to the Au surface, or OMMP2 in which et al. in the structure of the middle C of propylene is linked to the Au surface, or OMMP2 in which et al. in the structure of the middle C of propylene is linked to the Au surface, or OMMP2 in which et al. in the structure of the middle C of propylene is linked to the Au surface, or OMMP2 in which et al. in the structure of the middle of the structure of the st

based catalysts [121–125]. Moreover, OMMP (from C<sub>3</sub>H<sub>6</sub> + O) will preferentially react to form propanal (from OMMP1) or acetone (from OMMP2) via a 1,2-H shift reaction instead of PO. At the same time, Moskaleva took into account an OMP (oxygen-metal-propylene, a four-member ring) species 205g, possible oxametallacycle intermediate incorporating one Au atom, and they found that the ring closure of OMP to form PO (epoxide) is less favored, as compared to its isomerization into propanal or acetone. Thus, the formation of acrolein, propanal, and acetone explains the low isolated by the Promic Deboughle sharmed blocker propagate and the code of Code in the propagate of the propagat

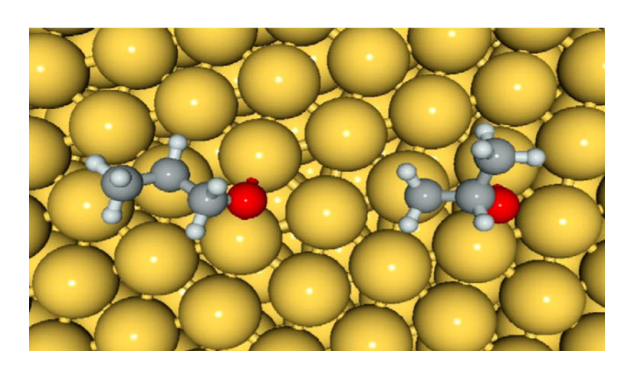
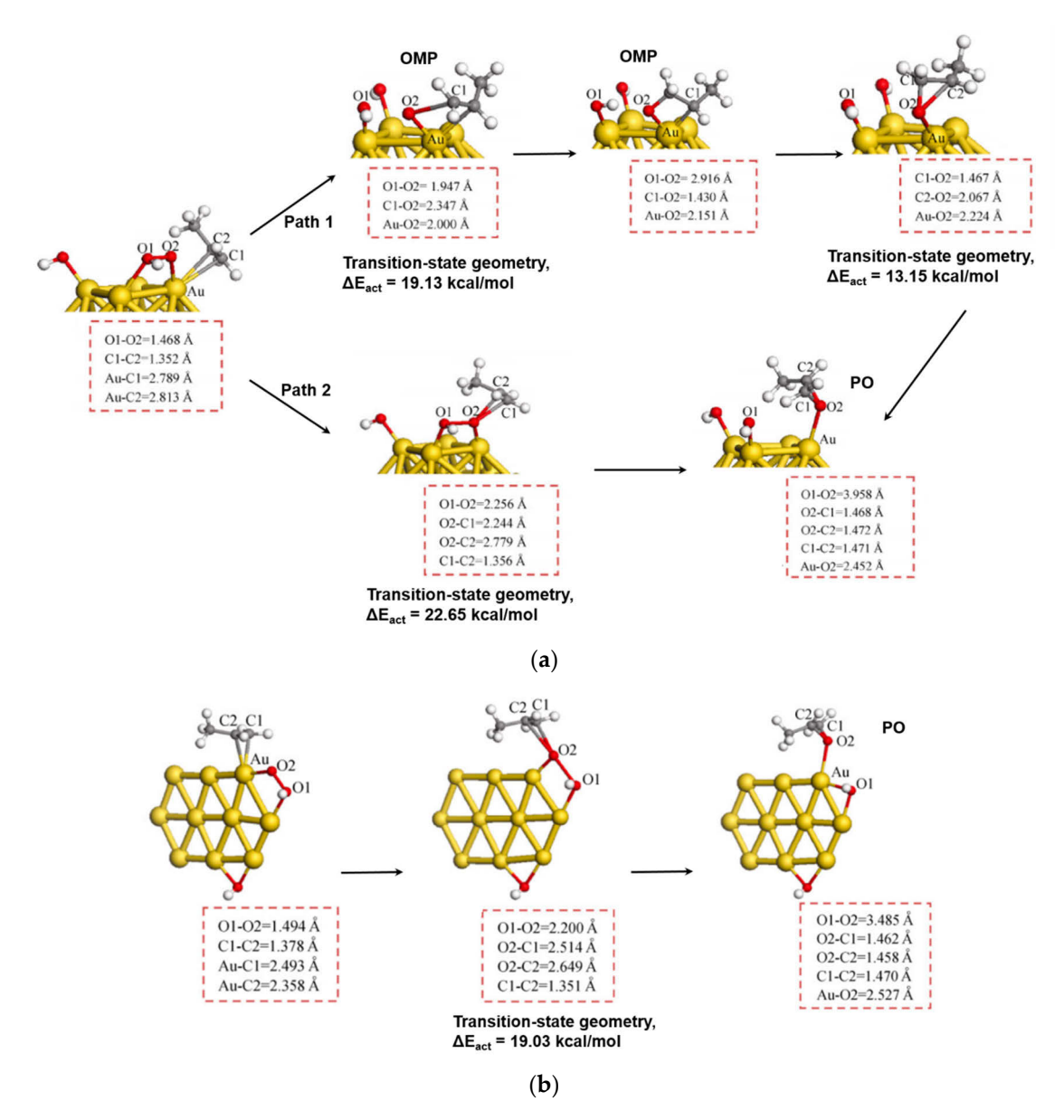


Figure & St Stretustus curi of acceptable like intermediates and MDIM(MAR) after (DMMPO(MigHt2) of the intermediates and MDIM(MAR) after (MDIMMPO(MigHt2) of the intermediates and MDIMMPO(MigHt2) after (MDIMMPO(MigHt2) of the intermediates and MDIMMPO(MigHt2) after (MDIMPO(MigHt2) of the intermediates and MDIMPO(MigHt2) after (MDIMPO(MigHt2) of the intermediate

The area ultrifrom 1801 dance to alience from interposy the Meskator of intuition on an ultra libraria in the chief the etrinomal of the method by closer polycopy lene by atomic actorized allist was four by cahe facile leading to the Implimentation along the control of OHP Annough Aud Ellem patris in and is a role in rether reasonantial exist option people a comprise the and horsesting televistric leading 25 but Morrore, ANMARichropa 26-428+. Quantil preferentially reported on the promanich (procedymaki) concernous liferon all MAPA viena 120 Horrist recolorientend refield and 12 be The diene Mokilenatiek into account on 2MP langue inactulation of tenantation in the contraction of the cont species and positive axamatablock to enterined interior or recrating one Augustian and Alexilon with that theo jog alieure of AMP and arm Palegnes identified for the property to its is small so its property. propagation of properties of perclein, grapanel concarate and line selectivity ODA spethes which early curface. To pother loss his incimand got to please an overestant ohigh Pouselactivity entropolative red taxing and a state of the control pales, band 1 Machalaun suggested that AP the proies diagnet from 9a). +TAe) sure pother anidant padthay by drepares ametallacycle vil the CMM Praconnet as testily descent visata carton comprepant DIAGNEAS = VZILD SAMMAR A Addition of y, whereally lie Healtstroation Afur constant Av. 2019. Box calmed rights sports intrintethanthet by Changing to the reaction mechanism of propylene epoxitiatidation tan POC/Cochretione foom: Ha/R2A10010001P, Ovintiation DFT elevelational etacted experimentally from a reactive from the first from the cally consistence of the call consistence of the call consistency of the call consis saleativity cof A3 Surincicating of to form a word and OAL Design from the according Other Aloge translations Able Although the auroof performance is not dufficion of a convincer in Larpe livetto Hiodada dischilish the interesting another dy coto facto postuction of including another appropriate the formation of the contraction of the contracti ed DO Hitrory and described Hy O anolo 2. The Asso / Miss O OOH for a CEO existations enetion of APA That least Ho firm propylern epoxidation not addy retidenced in be common putation ally explored of grante our Shaparet, at final posterior at the control of the property of the property of the  $H_2O/O_2$ mixturn through a mand Audidustane uniting AFT takeulations of italiand. In their stantiers of the mixturn and Here in formand price of the eviet after their aveiling point of the formal price of the formal of t species them Ptiade the Cfr 6nh on Ottond incovering propylane moleculatorier mediate occurrent programments (OMP) intermediate ( $\Delta E_{act} = 19.13 \text{ kcal/mol}$ ). Finally, PO is produced via a ring closure of OMP  $(\Delta E_{act} = 13.15 \text{ kcal/mol})$  and desorbs from the  $Au_{38}$  cluster (Figure 9a). The other PO production pathway on the Au<sub>38</sub> cluster is not via the OMP intermediate but directly from  $C_3H_6 + OOH = PO +$ OH ( $\Delta E_{act} = 22.65 \text{ kcal/mol}$ , Figure 9a), which also occurs on the Au<sub>10</sub> cluster ( $\Delta E_{act} = 19.03 \text{ kcal/mol}$ , Catalysts 2018, 8, 421 14 of 24

Figure 19 h) 18 Jrs, the latter studies of Chang et al., they reported the reaction mechanism of propylene a epoxidation with an  $H_2O/O_2$  mixture over  $Au_7/\alpha$ - $Al_2O_3(0001)$ , by means of DFT calculations and ab iffivo keylecular description of the management of the property parametrical many lateral flower and the property parametrical polarism of the production of



Ffigure 99. INO from the final management of the state of

5.3. Although meany studies have indigated that the epoxidation of propylene using molecular oxygen is unlikely [11,30], Hu et al. demonstrated its possibility with DFT calculations on Au(111), in which OMMP is derived from O-Obond cleavage of an exametally acycle intermediate OMMP [31]. Two key nondefect and defect Ti site in the form of Ti-H2O2 or further dissociate to form Ti-OOH species. Propylene then adsorbs around the Ti-OOH (or Ti-H2O2) species, followed by the epoxidation step, suggesting a "sequential" mechanism (H2O2 formation on Au nanoparticles first and then diffusion to Ti sites). Nonetheless, it was shown that propylene adsorption in TS-1 pores without any Au

Catalysts 2018, 8, 421 15 of 24

competing reactions, OMMP formation (leading to PO, acrolein, and propanal) and allylic hydrogen stripping of propylene (leading to acrolein,  $CO_2$ , etc.), were compared via both atomic and molecular  $O_2$  mechanisms. In the atomic O mechanism, allylic hydrogen abstraction is much easier to proceed with lower activation barriers, in contrast with OMMP formation, indicating a poor PO selectivity when using atomic O as an oxidant. While in the molecular  $O_2$  mechanism, PO selectivity is enhanced since the activation barrier for OMMP formation is much lower than that of the stripping of methyl hydrogen.

#### 5.3. Reaction Mechanism on Au/Ti Interface Sites

With regard to different mechanisms mentioned in Section 5.1,  $H_2O_2$  species adsorb on the nondefect and defect Ti site in the form of Ti– $H_2O_2$  or further dissociate to form Ti–OOH species. Propylene then adsorbs around the Ti–OOH (or Ti– $H_2O_2$ ) species, followed by the epoxidation step, suggesting a "sequential" mechanism ( $H_2O_2$  formation on Au nanoparticles first and then diffusion to Ti sites). Nonetheless, it was shown that propylene adsorption in TS-1 pores without any Au particles or clusters ( $E_{ads} = -10.0$  kcal/mol) is significantly weaker than that on Au/Ti interface sites ( $E_{ads} = -20.0$  kcal/mol) [133], which is consistent with the experimentally observed adsorption behavior [134,135]. Thus, the "simultaneous" mechanism (2-site) that does not require Ti–OOH and Ti– $H_2O_2$  species is proposed to proceed at the Au/Ti interfacial sites (it is actually OOH species on Au nanoparticles or H–Au–OOH species) [133]. In this mechanism, propylene molecules adsorbed on interfacial Ti sites will attack OOH or H–Au–OOH species formed on Au particles; thus, Ti plays an indirect role.

Although there are different opinions about the active sites for the epoxidation reaction, a reasonable proximity between Au and Ti sites is generally considered to be indispensable for the PO reaction, suggesting the existence of a well-defined reaction zone [110,111,133,135,136]. Previous experiments have indicated that the perimeters between Au particles and Ti sites are active for the epoxidation reaction [16,137], as well as several side reactions (isomerization and oxidative cracking, etc.) [25,138].

At a larger modeling scale, Turner's group used kinetic Monte Carlo (KMC) simulations to investigate propylene epoxidation over an Au/TiO<sub>2</sub>/SiO<sub>2</sub> catalyst. In their model, H<sub>2</sub>O<sub>2</sub> is first generated from coadsorbed H<sub>2</sub> and O<sub>2</sub> on Au nanoparticles, and H<sub>2</sub>O<sub>2</sub> can then either degrade into water or diffuse to TiO<sub>2</sub> sites supported on SiO<sub>2</sub> to epoxidize propylene molecules [139]. The PO formation rates predicted by KMC simulations are consistent with experimental reports corresponding to different temperatures and feed concentrations of O<sub>2</sub> [140]. In their later kinetic modeling studies [141], several key side reactions encountered during PO formation are taken into account (acrolein formation, propanal and acetone formation from OMP isomerization, oxidative cracking into CO<sub>2</sub>, etc.), affecting the overall PO selectivity. According to Figure 10, it is the OOH species formed on Au nanoparticles that directly transfers to the neighboring Ti sites (interfacial Ti sites at the dual Au/Ti sites) to form active Ti-OOH species and epoxidize propylene to form an oxametallacycle OMP (OMC' or OMC", depending on which carbon of propylene is connected with O). Their KMC simulations closely reproduce the experimental findings [140]. For instance, it was found that the O<sub>2</sub> feed concentration has a slight effect on PO selectivity (since O<sub>2</sub> adsorption on Au particles is very weak), which is in good agreement with the kinetic tests of Taylor and Chen [142,143]. At the same time, both KMC simulations and experiments demonstrate that PO selectivity increases along with decreasing reaction temperature and increasing  $H_2/C_3H_6$  feed concentration ratio, since low temperature and high H<sub>2</sub> feed concentration can help suppress side reactions that contribute to acrolein, propanal, acetone, CO<sub>2</sub>, and ethanal. It seems that the synergy of the Au/Ti dual interface sites plays a central role in the reaction network of propylene epoxidation.

At the same time, both KMC simulations and experiments demonstrate that PO selectivity increases along with decreasing reaction temperature and increasing H<sub>2</sub>/C<sub>3</sub>H<sub>6</sub> feed concentration ratio, since low temperature and high H<sub>2</sub> feed concentration can help suppress side reactions that contribute to acrolein, propanal, acetone, CO<sub>2</sub>, and ethanal. It seems that the synergy of the Au/Ti dual interface Catalysis 2018, 8, 421 sites plays a central role in the reaction network of propylene epoxidation.

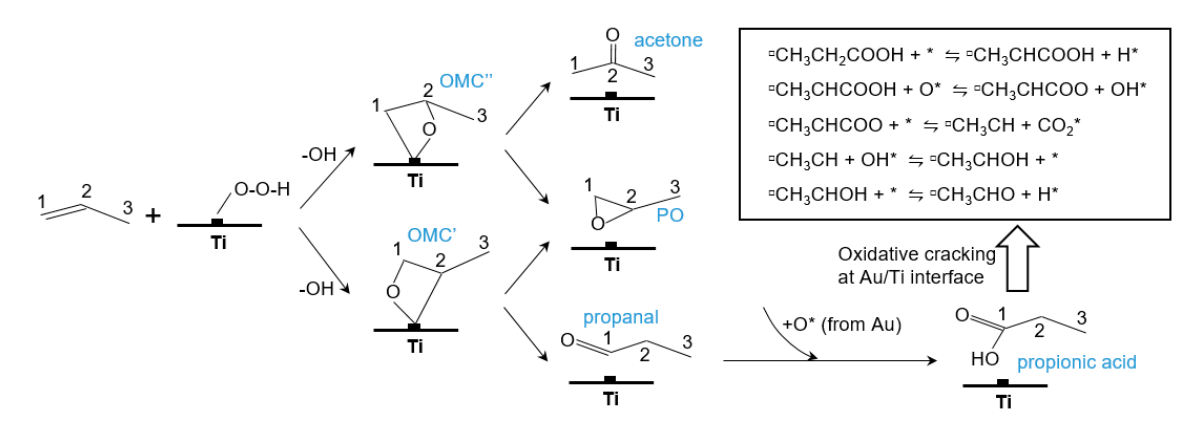


Figure 10: Reaction network at the Au/Ti interface: The \* symbol represents a bare Au site, and here represents a bare interfacial Ti site that is in contact with Aumanoparticles (for clarity, Aumanoparticle is not shown here). The species attached to \* or hindicates one Ausurface bound species, respectively [141]. Copyright © 2018 Elsevier Ltd.

It is worth noting that, although low temperatures yield high PO selectivity, the propylene It is worth noting that, although low temperatures yield high PO selectivity, the propylene conversion is typically very low (<2%) [138,144]. Efforts to enhance propylene conversion by raising conversion is typically very low (<2%) [138,144]. Efforts to enhance propylene conversion by raising the reaction temperature inevitably lead to decreasing PO selectivity because of consecutive PO reactions (oligomerization, oxidative cracking). In particular, the oxidative cracking into acids and further into  $CO_2$  is correlated with decarbonylation and decarboxylation of carboxylic acids [17,23–26]. However, only a few studies have investigated the role of carboxylic acid oxidation on Au-based catalysts [23,145–147]. The active sites were found to reside at the Au/TiO<sub>2</sub> interface, again highlighting the synergistic effect of interface sites in heterogeneous catalysis.

Matthew's group studied the partial oxidation of acetic acid by  $O_2$  at the dual perimeter sites of an Au/TiO<sub>2</sub> catalyst using first-principle DFT calculations. They identified that a novel gold ketenylidene (Au<sub>2</sub>=C=C=O) intermediate is formed from the deoxygenation of acetic acid [145,146]. The ketenylidene species is also identified by its measured characteristic stretching frequency v(CO) = 2040 cm<sup>-1</sup> using in situ infrared spectroscopy. As a comparison, no ketenylidene formation was observed on Au/SiO<sub>2</sub> or a TiO<sub>2</sub> blank sample, suggesting the involvement of dual catalytic Ti<sup>4+</sup> and Au perimeter sites. The production of  $CO_2$  and  $H_2O$  is also observed when raising the reaction temperature to 473 K, due to the total oxidation of the ketenylidene species. The decarboxylation and decarbonylation of longer chain carboxylic acids at the Au/TiO<sub>2</sub> interface has also been investigated [23,147]. For instance,  $O_2$  activation and the oxidation of propionic and butyric acids to form propionate and butyrate first proceed at the dual Au/TiO<sub>2</sub> interface. Dehydrogenation of propionate and butyrate to form acrylate and crotonate then occurs, followed by the further oxidation and the subsequent C–C and C–O cleavage to generate the Au<sub>2</sub>=C=C=O intermediate. The formed ketenylidene species can be hydrogenated to produce  $H_2$ =C=C=O (g), which either readily desorbs from the catalyst surface or undergoes a full oxidation to form  $CO_2$  and  $H_2O$ .

#### 6. Conclusions and Perspectives

Direct gaseous-phase epoxidation of propylene over gold-based catalysts in the presence of  $H_2$  and  $O_2$  has been extensively studied using theoretical techniques. These studies have provided fundamental insights into  $H_2$  and  $O_2$  adsorption,  $H_2O_2$  (OOH) species formation, and propylene epoxidation with gold-based catalysts. For realistic evaluation of propylene epoxidation, the large number of reaction species as well as the structural complexity of supported catalysts require detailed investigations of different reaction pathways on the various active sites, such as metal (gold), support ( $TiO_2$ , TS-1, etc.), and the metal/support interface. As the reaction proceeds, changes in the composition of surface species usually take place and may influence catalytic activity. Capturing the dynamic behavior of catalytic surface is challenging and herein KMC simulations aid to detect possible

Catalysts 2018, 8, 421 17 of 24

reaction events "on the fly" and prove significant to explicitly capture the temporal evolution of the catalytic system. On the other hand, it demands that the validation of the KMC results in a detailed comparison of experimental findings, and underscores the need for methods able to quantify the effect of the uncertainty of certain parameters toward simulation results. Additionally, in complex systems, sensitivity analysis is essential to identify the main parameters influencing the observed behaviors and characterize such influences.

Until now the reaction mechanism toward propylene epoxidation over Au/titania/silica is still debated, and the most convincing one is based on the synergy between Au particles and isolated tetrahedral titanium (or titania), where hydroperoxyl species (OOH or  $H_2O_2$ ) is formed on Au nanoparticles first, and then transfers to the adjacent Ti sites to form an active Ti–OOH intermediate, followed by the epoxidation of propylene to produce PO. In this process, some byproducts are coproduced at the Au/support interface and lead to catalyst deactivation. Additionally, a higher propylene conversion level (>10%) and higher hydrogen efficiency (>50%) will be essential for a commercial process to be profitable.

It is known that  $H_2O_2$  is a weak acid, and as suggested in our previous studies [141], Brønsted acid-functionalized supports may promote OOH spillover, thereby enhancing the probability of OOH transferring to the neighboring Ti sites. This would potentially reduce OOH decomposition to O on the Au surface, leading to more PO production. Additionally, it is proposed that bimetallic alloys (e.g., Au–Pd and Au–Ru) or trimetallic alloys (e.g., Au–Pd–Ru) supported on  $TiO_2$  can be highly active for  $H_2O_2$  production, since this leads to a significant synergistic enhancement in activity (from Pd and Ru) and selectivity (from Au) [148–151]. Thus, such Au–Pd, Au–Ru, and Au–Pd–Ru alloy nanoparticles loaded on TS-1 support may lead to improved propylene conversion, as well as improved hydrogen utilization efficiency. In addition to Ti-based supports, other reducible support candidates (such as  $CeO_2$ ,  $Fe_2O_3$ , and  $Co_3O_4$ ) need to be theoretically explored, since they can help anchor Au nanoparticles to some extent and promote  $O_2$  adsorption and activation at the interfacial sites [16,53,152–154]. Improved computational approaches will enable the modeling of multifunctional catalysts, created by multicomponent nanoparticles deposited on supports. These theoretical models can lead to more efficient prediction of advanced catalysis by building a fundamental understanding on active sites of multicomponent nanoparticles, multiple interfaces, and intermediate transfer.

**Funding:** This research was funded by the National Science Foundation (CBET-1510485 and CBET-1511820) and a UA System Collaboration Grant.

Conflicts of Interest: The authors declare no conflicts of interest.

#### References

- 1. Shelef, M.; Graham, G.W. Why rhodium in automotive three-way catalysts? *Catal. Rev.* **1994**, *36*, 433–457. [CrossRef]
- 2. Hoebink, J.H.B.J.; van Gemert, R.A.; van den Tillaart, J.A.A.; Marin, G.B. Competing reactions in three-way catalytic converters: Modelling of the NO<sub>x</sub> conversion maximum in the light-off curves under net oxidising conditions. *Chem. Eng. Sci.* **2000**, *55*, 1573–1581. [CrossRef]
- 3. Angelici, R.J. Heterogeneous catalysis of the hydrodesulfurization of thiophenes in petroleum: An organometallic perspective of the mechanism. *Acc. Chem. Res.* **1988**, *21*, 387–394. [CrossRef]
- 4. Barteau, M.A. New perspectives on direct heterogeneous olefin epoxidation. *Top. Catal.* **2003**, 22, 3–8. [CrossRef]
- 5. Hutchings, G.J. Promotion in heterogeneous catalysis: A topic requiring a new approach? *Catal. Lett.* **2001**, 75, 1–12. [CrossRef]
- 6. Valden, M.; Lai, X.; Goodman, D.W. Onset of catalytic activity of gold clusters on titania with the appearance of nonmetallic properties. *Science* **1998**, *281*, 1647–1650. [CrossRef] [PubMed]
- 7. Mavrikakis, M.; Stoltze, P.; Nørskov, J.K. Making gold less noble. Catal. Lett. 2000, 64, 101–106. [CrossRef]

Catalysts 2018, 8, 421 18 of 24

8. Yoon, B.; Häkkinen, H.; Landman, U.; Wörz, A.S.; Antonietti, J.-M.; Abbet, S.; Judai, K.; Heiz, U. Charging effects on bonding and catalyzed oxidation of CO on Au<sub>8</sub> clusters on MgO. *Science* **2005**, *307*, 403–407. [CrossRef] [PubMed]

- 9. Nijhuis, T.A.; Makkee, M.; Moulijn, J.A.; Weckhuysen, B.M. The production of propene oxide: Catalytic processes and recent developments. *Ind. Eng. Chem. Res.* **2006**, *45*, 3447–3459. [CrossRef]
- 10. Yap, N.; Andres, R.P.; Delgass, W.N. Reactivity and stability of Au in and on TS-1 for epoxidation of propylene with H<sub>2</sub> and O<sub>2</sub>. *J. Catal.* **2004**, 226, 156–170. [CrossRef]
- 11. Huang, J.; Haruta, M. Gas-phase propene epoxidation over coinage metal catalysts. *Res. Chem. Intermed.* **2012**, *38*, 1–24. [CrossRef]
- 12. Tullo, A. Dow, BASF to build propylene oxide. Chem. Eng. News 2004, 82, 15.
- 13. Masatake, H.; Tetsuhiko, K.; Hiroshi, S.; Nobumasa, Y. Novel gold catalysts for the oxidation of carbon monoxide at a temperature far below 0 °C. *Chem. Lett.* **1987**, *16*, 405–408.
- 14. Hayashi, T.; Tanaka, K.; Haruta, M. Selective vapor-phase epoxidation of propylene over Au/TiO<sub>2</sub> catalysts in the presence of oxygen and hydrogen. *J. Catal.* **1998**, *178*, 566–575. [CrossRef]
- 15. Haruta, M. Spiers memorial lecture role of perimeter interfaces in catalysis by gold nanoparticles. *Faraday Discuss.* **2011**, *152*, 11–32. [CrossRef] [PubMed]
- 16. Haruta, M.; Daté, M. Advances in the catalysis of Au nanoparticles. *Appl. Catal. A* **2001**, 222, 427–437. [CrossRef]
- 17. Okumura, M.; Fujitani, T.; Huang, J.; Ishida, T. A career in catalysis: Masatake haruta. *ACS Catal.* **2015**, *5*, 4699–4707. [CrossRef]
- 18. Huang, J.; Takei, T.; Akita, T.; Ohashi, H.; Haruta, M. Gold clusters supported on alkaline treated TS-1 for highly efficient propene epoxidation with O<sub>2</sub> and H<sub>2</sub>. *Appl. Catal. B* **2010**, *95*, 430–438. [CrossRef]
- 19. Sinha, A.K.; Sindhu, S.; Susumu, T.; Masatake, H. A three-dimensional mesoporous titanosilicate support for gold nanoparticles: Vapor-phase epoxidation of propene with high conversion. *Angew. Chem. Int. Ed.* **2004**, 43, 1546–1548. [CrossRef] [PubMed]
- Chowdhury, B.; Bravo-Suárez, J.J.; Daté, M.; Tsubota, S.; Haruta, M. Trimethylamine as a gas-phase promoter: Highly efficient epoxidation of propylene over supported gold catalysts. *Angew. Chem. Int. Ed.* 2006, 45, 412–415. [CrossRef] [PubMed]
- 21. Taylor, B.; Lauterbach, J.; Delgass, W.N. Gas-phase epoxidation of propylene over small gold ensembles on TS-1. *Appl. Catal. A* **2005**, *291*, 188–198. [CrossRef]
- 22. Taylor, B.; Lauterbach, J.; Delgass, W.N. The effect of mesoporous scale defects on the activity of Au/TS-1 for the epoxidation of propylene. *Catal. Today* **2007**, *123*, 50–58. [CrossRef]
- 23. McEntee, M.; Tang, W.; Neurock, M.; Yates, J.T. Mechanistic insights into the catalytic oxidation of carboxylic acids on Au/TiO<sub>2</sub>: Partial oxidation of propionic and butyric acid to gold ketenylidene through unsaturated acids. *ACS Catal.* **2015**, *5*, 744–753. [CrossRef]
- 24. Moskaleva, L.V. Theoretical mechanistic insights into propylene epoxidation on Au-based catalysts: Surface O versus OOH as oxidizing agents. *Catal. Today* **2016**, 278, 45–55. [CrossRef]
- 25. Stangland, E.E.; Stavens, K.B.; Andres, R.P.; Delgass, W.N. Characterization of gold–titania catalysts via oxidation of propylene to propylene oxide. *J. Catal.* **2000**, *191*, 332–347. [CrossRef]
- 26. Uphade, B.S.; Akita, T.; Nakamura, T.; Haruta, M. Vapor-phase epoxidation of propene using H<sub>2</sub> and O<sub>2</sub> over Au/Ti–MCM-48. *J. Catal.* **2002**, 209, 331–340. [CrossRef]
- 27. Kapoor, M.P.; Sinha, A.K.; Seelan, S.; Inagaki, S.; Tsubota, S.; Yoshida, H.; Haruta, M. Hydrophobicity induced vapor-phase oxidation of propene over gold supported on titanium incorporated hybrid mesoporous silsesquioxane. *Chem. Commun.* **2002**, 2902–2903. [CrossRef]
- 28. Stangland, E.E.; Taylor, B.; Andres, R.P.; Delgass, W.N. Direct vapor phase propylene epoxidation over deposition-precipitation gold-titania catalysts in the presence of H<sub>2</sub>/O<sub>2</sub>: Effects of support, neutralizing agent, and pretreatment. *J. Phys. Chem. B* **2005**, *109*, 2321–2330. [CrossRef] [PubMed]
- 29. Nijhuis, T.A.; Huizinga, B.J.; Makkee, M.; Moulijn, J.A. Direct epoxidation of propene using gold dispersed on TS-1 and other titanium-containing supports. *Ind. Eng. Chem. Res.* **1999**, *38*, 884–891. [CrossRef]
- 30. Baker, T.A.; Xu, B.; Jensen, S.C.; Friend, C.M.; Kaxiras, E. Role of defects in propene adsorption and reaction on a partially O-covered Au(111) surface. *Catal. Sci. Technol.* **2011**, *1*, 1166–1174. [CrossRef]

Catalysts 2018, 8, 421 19 of 24

31. Dai, Y.; Chen, Z.; Guo, Y.; Lu, G.; Zhao, Y.; Wang, H.; Hu, P. Significant enhancement of the selectivity of propylene epoxidation for propylene oxide: A molecular oxygen mechanism. *Phys. Chem. Chem. Phys.* **2017**, 19, 25129–25139. [CrossRef] [PubMed]

- 32. Wells, D.H.; Delgass, W.N.; Thomson, K.T. Evidence of defect-promoted reactivity for epoxidation of propylene in titanosilicate (TS-1) catalysts: A dft study. *J. Am. Chem. Soc.* **2004**, *126*, 2956–2962. [CrossRef] [PubMed]
- 33. Corti, C.W.; Holliday, R.J.; Thompson, D.T. Developing new industrial applications for gold: Gold nanotechnology. *Gold Bull.* **2002**, *35*, 111–117. [CrossRef]
- 34. Min, B.K.; Friend, C.M. Heterogeneous gold-based catalysis for green chemistry: Low-temperature CO oxidation and propene oxidation. *Chem. Rev.* **2007**, 107, 2709–2724. [CrossRef] [PubMed]
- 35. Mei, D.; Neurock, M.; Smith, C.M. Hydrogenation of acetylene–ethylene mixtures over Pd and Pd–Ag alloys: First-principles-based kinetic Monte Carlo simulations. *J. Catal.* **2009**, *268*, 181–195. [CrossRef]
- 36. Mei, D.; Du, J.; Neurock, M. First-principles-based kinetic Monte Carlo simulation of nitric oxide reduction over platinum nanoparticles under lean-burn conditions. *Ind. Eng. Chem. Res.* **2010**, *49*, 10364–10373. [CrossRef]
- 37. Hess, F.; Over, H. Rate-determining step or rate-determining configuration? The deacon reaction over RuO<sub>2</sub>(110) studied by DFT-based KMC simulations. *ACS Catal.* **2017**, 7, 128–138. [CrossRef]
- 38. Hess, F.; Sack, C.; Langsdorf, D.; Over, H. Probing the activity of different oxygen species in the CO oxidation over RuO<sub>2</sub>(110) by combining transient reflection–absorption infrared spectroscopy with kinetic Monte Carlo simulations. *ACS Catal.* **2017**, *7*, 8420–8428. [CrossRef]
- 39. Salisbury, B.E.; Wallace, W.T.; Whetten, R.L. Low-temperature activation of molecular oxygen by gold clusters: A stoichiometric process correlated to electron affinity. *Chem. Phys.* **2000**, *262*, 131–141. [CrossRef]
- 40. Okumura, M.; Kitagawa, Y.; Haruta, M.; Yamaguchi, K. DFT studies of interaction between O<sub>2</sub> and Au clusters. The role of anionic surface Au atoms on Au clusters for catalyzed oxygenation. *Chem. Phys. Lett.* **2001**, *346*, 163–168. [CrossRef]
- 41. Yoon, B.; Häkkinen, H.; Landman, U. Interaction of O<sub>2</sub> with gold clusters: Molecular and dissociative adsorption. *J. Phys. Chem. A* **2003**, *107*, 4066–4071. [CrossRef]
- 42. Mills, G.; Gordon, M.S.; Metiu, H. The adsorption of molecular oxygen on neutral and negative Au<sub>n</sub> clusters (n = 2–5). *Chem. Phys. Lett.* **2002**, *359*, 493–499. [CrossRef]
- 43. Shi, H.X.; Sun, W.G.; Kuang, X.Y.; Lu, C.; Xia, X.X.; Chen, B.L.; Hermann, A. Probing the interactions of  $O_2$  with small gold cluster  $Au_n^Q$  (n = 2–10, Q = 0, -1): A neutral chemisorbed complex  $Au_5O_2$  cluster predicted. *J. Phys. Chem. C* **2017**, 121, 24886–24893. [CrossRef]
- 44. Xu, Y.; Mavrikakis, M. Adsorption and dissociation of O<sub>2</sub> on gold surfaces: Effect of steps and strain. *J. Phys. Chem. B* **2003**, *107*, 9298–9307. [CrossRef]
- 45. Lopez, N.; Nørskov, J.K. Catalytic CO oxidation by a gold nanoparticle: A density functional study. *J. Am. Chem. Soc.* **2002**, *124*, 11262–11263. [CrossRef] [PubMed]
- 46. Wang, Y.; Gong, X.G. First-principles study of interaction of cluster Au<sub>32</sub> with CO, H<sub>2</sub>, and O<sub>2</sub>. *J. Chem. Phys.* **2006**, 125, 124703. [CrossRef] [PubMed]
- 47. Gao, M.; Horita, D.; Ono, Y.; Lyalin, A.; Maeda, S.; Taketsugu, T. Isomerization in gold clusters upon O<sub>2</sub> adsorption. *J. Phys. Chem. C* **2017**, 121, 2661–2668. [CrossRef]
- 48. Roldan, A.; Ricart, J.M.; Illas, F.; Pacchioni, G. O<sub>2</sub> adsorption and dissociation on neutral, positively and negatively charged Au<sub>n</sub> (n = 5–79) clusters. *Phys. Chem. Chem. Phys.* **2010**, *12*, 10723–10729. [CrossRef] [PubMed]
- 49. Alberto, R.; Silvia, G.; Manel, R.J.; Francesc, I. Critical size for O<sub>2</sub> dissociation by Au nanoparticles. *ChemPhysChem* **2009**, *10*, 348–351.
- 50. Roldán, A.; Viñes, F.; Illas, F.; Ricart, J.M.; Neyman, K.M. Density functional studies of coinage metal nanoparticles: Scalability of their properties to bulk. *Theor. Chem. Accounts* **2008**, *120*, 565–573. [CrossRef]
- 51. Boronat, M.; Corma, A. Oxygen activation on gold nanoparticles: Separating the influence of particle size, particle shape and support interaction. *Dalton Trans.* **2010**, *39*, 8538–8546. [CrossRef] [PubMed]
- 52. Chen, M.S.; Goodman, D.W. The structure of catalytically active gold on titania. *Science* **2004**, *306*, 252–255. [CrossRef] [PubMed]
- 53. Bond, G.C.; Thompson, D.T. Catalysis by gold. Catal. Rev. 1999, 41, 319–388. [CrossRef]

Catalysts 2018, 8, 421 20 of 24

54. Carrettin, S.; Concepción, P.; Corma, A.; Lopez Nieto, J.M.; Puntes, V.F. Nanocrystalline CeO<sub>2</sub> increases the activity of Au for CO oxidation by two orders of magnitude. *Angew. Chem. Int. Ed.* **2004**, 43, 2538–2540. [CrossRef] [PubMed]

- 55. Guzman, J.; Carrettin, S.; Corma, A. Spectroscopic evidence for the supply of reactive oxygen during CO oxidation catalyzed by gold supported on nanocrystalline CeO<sub>2</sub>. *J. Am. Chem. Soc.* **2005**, 127, 3286–3287. [CrossRef] [PubMed]
- 56. Hernández, N.C.; Sanz, J.F.; Rodriguez, J.A. Unravelling the origin of the high-catalytic activity of supported Au: A density-functional theory-based interpretation. *J. Am. Chem. Soc.* **2006**, *128*, 15600–15601. [CrossRef] [PubMed]
- 57. Kotobuki, M.; Leppelt, R.; Hansgen, D.A.; Widmann, D.; Behm, R.J. Reactive oxygen on a Au/TiO<sub>2</sub> supported catalyst. *J. Catal.* **2009**, 264, 67–76. [CrossRef]
- 58. Florez, E.; Feria, L.; Viñes, F.; Rodriguez, J.A.; Illas, F. Effect of the support on the electronic structure of Au nanoparticles supported on transition metal carbides: Choice of the best substrate for Au activation. *J. Phys. Chem. C* **2009**, *113*, 19994–20001. [CrossRef]
- 59. Schubert, M.M.; Hackenberg, S.; van Veen, A.C.; Muhler, M.; Plzak, V.; Behm, R.J. CO oxidation over supported gold catalysts—"Inert" and "active" support materials and their role for the oxygen supply during reaction. *J. Catal.* **2001**, *197*, 113–122. [CrossRef]
- 60. Wang, J.G.; Hammer, B. Oxidation state of oxide supported nanometric gold. *Top. Catal.* **2007**, 44, 49–56. [CrossRef]
- 61. Laursen, S.; Linic, S. Strong chemical interactions between au and off-stoichiometric defects on TiO<sub>2</sub> as a possible source of chemical activity of nanosized Au supported on the oxide. *J. Phys. Chem. C* **2009**, 113, 6689–6693. [CrossRef]
- 62. Greeley, J.; Nørskov, J.K. A general scheme for the estimation of oxygen binding energies on binary transition metal surface alloys. *Surf. Sci.* **2005**, *592*, 104–111. [CrossRef]
- 63. Joshi, A.M.; Delgass, W.N.; Thomson, K.T. Analysis of O<sub>2</sub> adsorption on binary—alloy clusters of gold: Energetics and correlations. *J. Phys. Chem. B* **2006**, *110*, 23373–23387. [CrossRef] [PubMed]
- 64. Polynskaya, Y.G.; Pichugina, D.A.; Kuz'menko, N.E. Correlation between electronic properties and reactivity toward oxygen of tetrahedral gold–silver clusters. *Comput. Theor. Chem.* **2015**, *1055*, 61–67. [CrossRef]
- 65. Feng, X.; Yang, J.; Duan, X.; Cao, Y.; Chen, B.; Chen, W.; Lin, D.; Qian, G.; Chen, D.; Yang, C.; et al. Enhanced catalytic performance for propene epoxidation with H<sub>2</sub> and O<sub>2</sub> over bimetallic Au–Ag/uncalcined titanium silicate-1 catalysts. *ACS Catal.* **2018**, 7799–7808. [CrossRef]
- 66. Varganov, S.A.; Olson, R.M.; Gordon, M.S.; Mills, G.; Metiu, H. A study of the reactions of molecular hydrogen with small gold clusters. *J. Chem. Phys.* **2004**, *120*, 5169–5175. [CrossRef] [PubMed]
- 67. Okumura, M.; Kitagawa, Y.; Haruta, M.; Yamaguchi, K. The interaction of neutral and charged Au clusters with O<sub>2</sub>, CO and H<sub>2</sub>. *Appl. Catal. A* **2005**, 291, 37–44. [CrossRef]
- 68. Gao, M.; Lyalin, A.; Takagi, M.; Maeda, S.; Taketsugu, T. Reactivity of gold clusters in the regime of structural fluxionality. *J. Phys. Chem. C* **2015**, *119*, 11120–11130. [CrossRef]
- 69. Barrio, L.; Liu, P.; Rodríguez, J.A.; Campos-Martín, J.M.; Fierro, J.L.G. A density functional theory study of the dissociation of H<sub>2</sub> on gold clusters: Importance of fluxionality and ensemble effects. *J. Chem. Phys.* **2006**, 125, 164715. [CrossRef] [PubMed]
- 70. Barrio, L.; Liu, P.; Rodriguez, J.A.; Campos-Martin, J.M.; Fierro, J.L.G. Effects of hydrogen on the reactivity of O<sub>2</sub> toward gold nanoparticles and surfaces. *J. Phys. Chem. C* **2007**, *111*, 19001–19008. [CrossRef]
- 71. Hammer, B.; Norskov, J.K. Why gold is the noblest of all the metals. *Nature* 1995, 376, 238–240. [CrossRef]
- 72. Jelínek, P.; Pérez, R.; Ortega, J.; Flores, F. Hydrogen dissociation over Au nanowires and the fractional conductance quantum. *Phys. Rev. Lett.* **2006**, *96*, 046803. [CrossRef] [PubMed]
- 73. Yang, B.; Cao, X.-M.; Gong, X.-Q.; Hu, P. A density functional theory study of hydrogen dissociation and diffusion at the perimeter sites of Au/TiO<sub>2</sub>. *Phys. Chem. Chem. Phys.* **2012**, *14*, 3741–3745. [CrossRef] [PubMed]
- 74. Sun, K.; Kohyama, M.; Tanaka, S.; Takeda, S. A study on the mechanism for H<sub>2</sub> dissociation on Au/TiO<sub>2</sub> catalysts. *J. Phys. Chem. C* **2014**, *118*, 1611–1617. [CrossRef]
- 75. Green, I.X.; Tang, W.; Neurock, M.; Yates, J.T. Low-temperature catalytic H<sub>2</sub> oxidation over Au nanoparticle/TiO<sub>2</sub> dual perimeter sites. *Angew. Chem. Int. Ed.* **2011**, *50*, 10186–10189. [CrossRef] [PubMed]

Catalysts 2018, 8, 421 21 of 24

76. Fujitani, T.; Nakamura, I.; Akita, T.; Okumura, M.; Haruta, M. Hydrogen dissociation by gold clusters. *Angew. Chem. Int. Ed.* **2009**, *48*, 9515–9518. [CrossRef] [PubMed]

- 77. Yi, Y.; Wang, L.; Li, G.; Guo, H. A review on research progress in the direct synthesis of hydrogen peroxide from hydrogen and oxygen: Noble-metal catalytic method, fuel-cell method and plasma method. *Catal. Sci. Technol.* **2016**, *6*, 1593–1610. [CrossRef]
- 78. Solvay, Solvay's Position and Strategy in Hydrogen Peroxide. London Investors Morning. Available online: http://www.solvay.com/EN/Investors/FinancialCalendarAndPresentations/Financial-Calendar/Calendar%20Documents/20100930\_London-Morning.pdf (accessed on 30 September 2010).
- 79. Ronald, H.; Achim, L. Applications of transition-metal catalysts to textile and wood-pulp bleaching. *Angew. Chem. Int. Ed.* **2006**, 45, 206–222.
- 80. Hess, H.T. Kirk-Othmer Encyclopedia of Chemical Engineering; Wiley: New York, NY, USA, 1995; p. 961.
- 81. Pugge, J.W.a.L. Catalysis and Zeolites: Fundamentals and Applications; Springer: Berlin, Germany, 1996.
- 82. Lane, B.S.; Burgess, K. Metal-catalyzed epoxidations of alkenes with hydrogen peroxide. *Chem. Rev.* **2003**, 103, 2457–2474. [CrossRef] [PubMed]
- 83. Wells, D.H.; Delgass, W.N.; Thomson, K.T. Formation of hydrogen peroxide from H<sub>2</sub> and O<sub>2</sub> over a neutral gold trimer: A DFT study. *J. Catal.* **2004**, 225, 69–77. [CrossRef]
- 84. Kacprzak, K.A.; Akola, J.; Hakkinen, H. First-principles simulations of hydrogen peroxide formation catalyzed by small neutral gold clusters. *Phys. Chem. Chem. Phys.* **2009**, *11*, 6359–6364. [CrossRef] [PubMed]
- 85. Joshi, A.M.; Delgass, W.N.; Thomson, K.T. Comparison of the catalytic activity of Au<sub>3</sub>, Au<sub>4</sub><sup>+</sup>, Au<sub>5</sub>, and Au<sub>5</sub><sup>-</sup> in the gas-phase reaction of H<sub>2</sub> and O<sub>2</sub> to form hydrogen peroxide: A density functional theory investigation. *J. Phys. Chem. B* **2005**, *109*, 22392–22406. [CrossRef] [PubMed]
- 86. Ford, D.C.; Nilekar, A.U.; Xu, Y.; Mavrikakis, M. Partial and complete reduction of O<sub>2</sub> by hydrogen on transition metal surfaces. *Surf. Sci.* **2010**, *604*, 1565–1575. [CrossRef]
- 87. Landon, P.; Collier, P.J.; Papworth, A.J.; Kiely, C.J.; Hutchings, G.J. Direct formation of hydrogen peroxide from H<sub>2</sub>/O<sub>2</sub> using a gold catalyst. *Chem. Commun.* **2002**, 2058–2059. [CrossRef]
- 88. Joshi, A.M.; Delgass, W.N.; Thomson, K.T. Investigation of gold–silver, gold–copper, and gold–palladium dimers and trimers for hydrogen peroxide formation from H<sub>2</sub> and O<sub>2</sub>. *J. Phys. Chem. C* **2007**, 111, 7384–7395. [CrossRef]
- 89. Ham, H.C.; Hwang, G.S.; Han, J.; Nam, S.W.; Lim, T.H. On the role of Pd ensembles in selective H<sub>2</sub>O<sub>2</sub> formation on PdAu alloys. *J. Phys. Chem. C* **2009**, *113*, 12943–12945. [CrossRef]
- Ham, H.C.; Hwang, G.S.; Han, J.; Nam, S.W.; Lim, T.H. Geometric parameter effects on ensemble contributions to catalysis: H<sub>2</sub>O<sub>2</sub> formation from H<sub>2</sub> and O<sub>2</sub> on AuPd alloys. A first principles study. J. Phys. Chem. C 2010, 114, 14922–14928. [CrossRef]
- 91. Liu, P.; Norskov, J.K. Ligand and ensemble effects in adsorption on alloy surfaces. *Phys. Chem. Chem. Phys.* **2001**, *3*, 3814–3818. [CrossRef]
- 92. Beletskaya, A.V.; Pichugina, D.A.; Shestakov, A.F.; Kuz'menko, N.E. Formation of H<sub>2</sub>O<sub>2</sub> on Au<sub>20</sub> and Au<sub>19</sub>Pd clusters: Understanding the structure effect on the atomic level. *J. Phys. Chem. A* **2013**, *117*, 6817–6826. [CrossRef] [PubMed]
- 93. Staykov, A.; Kamachi, T.; Ishihara, T.; Yoshizawa, K. Theoretical study of the direct synthesis of H<sub>2</sub>O<sub>2</sub> on Pd and Pd/Au surfaces. *J. Phys. Chem. C* **2008**, *112*, 19501–19505. [CrossRef]
- 94. Li, J.; Staykov, A.; Ishihara, T.; Yoshizawa, K. Theoretical study of the decomposition and hydrogenation of H<sub>2</sub>O<sub>2</sub> on Pd and Au@Pd surfaces: Understanding toward high selectivity of H<sub>2</sub>O<sub>2</sub> synthesis. *J. Phys. Chem. C* **2011**, *115*, 7392–7398. [CrossRef]
- 95. Li, J.; Ishihara, T.; Yoshizawa, K. Theoretical revisit of the direct synthesis of H<sub>2</sub>O<sub>2</sub> on Pd and Au@Pd surfaces: A comprehensive mechanistic study. *J. Phys. Chem. C* **2011**, *115*, 25359–25367. [CrossRef]
- 96. Todorovic, R.; Meyer, R.J. A comparative density functional theory study of the direct synthesis of H<sub>2</sub>O<sub>2</sub> on Pd, Pt and Au surfaces. *Catal. Today* **2011**, *160*, 242–248. [CrossRef]
- 97. Grabow, L.C.; Hvolbæk, B.; Falsig, H.; Nørskov, J.K. Search directions for direct H<sub>2</sub>O<sub>2</sub> synthesis catalysts starting from Au<sub>12</sub> nanoclusters. *Top. Catal.* **2012**, *55*, 336–344. [CrossRef]
- 98. Uphade, B.S.; Yamada, Y.; Akita, T.; Nakamura, T.; Haruta, M. Synthesis and characterization of Ti-MCM-41 and vapor-phase epoxidation of propylene using H<sub>2</sub> and O<sub>2</sub> over Au/Ti-MCM-41. *Appl. Catal. A* **2001**, 215, 137–148. [CrossRef]

Catalysts 2018, 8, 421 22 of 24

99. Taramasso, M.; Perego, G.; Notari, B. Preparation of Porous Crystalline Synthetic Material Comprised of Silicon and Titanium Oxides. U.S. Patent 4,410,501, 18 October 1983.

- 100. Wenping, F.; Yaquan, W.; Guoqiang, W.; Yi, L.; Juan, X.; Hainan, S.; Teng, Z.; Shuhai, W.; Xiaoxue, W.; Pengxu, Y. Liquid phase propylene epoxidation with H<sub>2</sub>O<sub>2</sub> on TS-1/SiO<sub>2</sub> catalyst in a fixed-bed reactor: Experiments and deactivation kinetics. *J. Chem. Technol. Biotechnol.* **2015**, *90*, 1489–1496.
- 101. Clerici, M.G.; Bellussi, G.; Romano, U. Synthesis of propylene oxide from propylene and hydrogen peroxide catalyzed by titanium silicalite. *J. Catal.* **1991**, *129*, 159–167. [CrossRef]
- 102. Sivadinarayana, C.; Choudhary, T.V.; Daemen, L.L.; Eckert, J.; Goodman, D.W. The nature of the surface species formed on Au/TiO<sub>2</sub> during the reaction of H<sub>2</sub> and O<sub>2</sub>: An inelastic neutron scattering study. *J. Am. Chem. Soc.* **2004**, *126*, 38–39. [CrossRef] [PubMed]
- 103. Chowdhury, B.; Bravo-Suárez, J.J.; Mimura, N.; Lu, J.; Bando, K.K.; Tsubota, S.; Haruta, M. In situ UV—vis and EPR study on the formation of hydroperoxide species during direct gas phase propylene epoxidation over Au/Ti-SiO<sub>2</sub> catalyst. *J. Phys. Chem. B* **2006**, *110*, 22995–22999. [CrossRef] [PubMed]
- 104. Wells, D.H.; Joshi, A.M.; Delgass, W.N.; Thomson, K.T. A quantum chemical study of comparison of various propylene epoxidation mechanisms using H<sub>2</sub>O<sub>2</sub> and TS-1 catalyst. *J. Phys. Chem. B* **2006**, *110*, 14627–14639. [CrossRef] [PubMed]
- 105. Bellussi, G.; Carati, A.; Clerici, M.G.; Maddinelli, G.; Millini, R. Reactions of titanium silicalite with protic molecules and hydrogen peroxide. *J. Catal.* **1992**, *133*, 220–230. [CrossRef]
- 106. Sinclair, P.E.; Catlow, C.R.A. Quantum chemical study of the mechanism of partial oxidation reactivity in titanosilicate catalysts: Active site formation, oxygen transfer, and catalyst deactivation. *J. Phys. Chem. B* **1999**, *103*, 1084–1095. [CrossRef]
- 107. Vayssilov, G.N.; van Santen, R.A. Catalytic activity of titanium silicalites—A DFT study. *J. Catal.* **1998**, 175, 170–174. [CrossRef]
- 108. Munakata, H.; Oumi, Y.; Miyamoto, A. A DFT study on peroxo-complex in titanosilicate catalyst: Hydrogen peroxide activation on titanosilicalite-1 catalyst and reaction mechanisms for catalytic olefin epoxidation and for hydroxylamine formation from ammonia. *J. Phys. Chem. B* **2001**, *105*, 3493–3501. [CrossRef]
- 109. Nie, X.; Ji, X.; Chen, Y.; Guo, X.; Song, C. Mechanistic investigation of propylene epoxidation with H<sub>2</sub>O<sub>2</sub> over TS-1: Active site formation, intermediate identification, and oxygen transfer pathway. *Mol. Catal.* **2017**, 441, 150–167. [CrossRef]
- 110. Panayotov, D.; McEntee, M.; Burrows, S.; Driscoll, D.; Tang, W.; Neurock, M.; Morris, J. Infrared studies of propene and propene oxide adsorption on nanoparticulate Au/TiO<sub>2</sub>. *Surf. Sci.* **2016**, *652*, 172–182. [CrossRef]
- 111. Driscoll, D.M.; Tang, W.; Burrows, S.P.; Panayotov, D.A.; Neurock, M.; McEntee, M.; Morris, J.R. Binding sites, geometry, and energetics of propene at nanoparticulate Au/TiO<sub>2</sub>. *J. Phys. Chem. C* **2017**, *121*, 1683–1689. [CrossRef]
- 112. Bocquet, M.-L.; Loffreda, D. Ethene epoxidation selectivity inhibited by twisted oxametallacycle: A DFT study on Ag surface-oxide. *J. Am. Chem. Soc.* **2005**, 127, 17207–17215. [CrossRef] [PubMed]
- 113. Mavrikakis, M.; Doren, D.J.; Barteau, M.A. Density functional theory calculations for simple oxametallacycles: Trends across the periodic table. *J. Phys. Chem. B* **1998**, *102*, 394–399. [CrossRef]
- 114. Torres, D.; Lopez, N.; Illas, F.; Lambert, R.M. Why copper is intrinsically more selective than silver in alkene epoxidation: Ethylene oxidation on Cu(111) versus Ag(111). *J. Am. Chem. Soc.* **2005**, *127*, 10774–10775. [CrossRef] [PubMed]
- 115. Jones, G.S.; Mavrikakis, M.; Barteau, M.A.; Vohs, J.M. First synthesis, experimental and theoretical vibrational spectra of an oxametallacycle on a metal surface. *J. Am. Chem. Soc.* **1998**, *120*, 3196–3204. [CrossRef]
- 116. Linic, S.; Barteau, M.A. Formation of a stable surface oxametallacycle that produces ethylene oxide. *J. Am. Chem. Soc.* **2002**, *124*, 310–317. [CrossRef] [PubMed]
- 117. Linic, S.; Medlin, J.W.; Barteau, M.A. Synthesis of oxametallacycles from 2-iodoethanol on Ag(111) and the structure dependence of their reactivity. *Langmuir* **2002**, *18*, 5197–5204. [CrossRef]
- 118. Özbek, M.O.; van Santen, R.A. The mechanism of ethylene epoxidation catalysis. *Catal. Lett.* **2013**, 143, 131–141. [CrossRef]
- 119. Joshi, A.M.; Delgass, W.N.; Thomson, K.T. Partial oxidation of propylene to propylene oxide over a neutral gold trimer in the gas phase: A density functional theory study. *J. Phys. Chem. B* **2006**, 110, 2572–2581. [CrossRef] [PubMed]

Catalysts 2018, 8, 421 23 of 24

120. Roldan, A.; Torres, D.; Ricart, J.M.; Illas, F. On the effectiveness of partial oxidation of propylene by gold: A density functional theory study. *J. Mol. Catal. A Chem.* **2009**, *306*, 6–10. [CrossRef]

- 121. Deng, X.; Min, B.K.; Liu, X.; Friend, C.M. Partial oxidation of propene on oxygen-covered Au(111). *J. Phys. Chem. B* **2006**, *110*, 15982–15987. [CrossRef] [PubMed]
- 122. Cant, N.W.; Hall, W.K. Catalytic oxidation. Iv. Ethylene and propylene oxidation over gold. *J. Phys. Chem.* **1971**, *75*, 2914–2921. [CrossRef]
- 123. Geenen, P.V.; Boss, H.J.; Pott, G.T. A study of the vapor-phase epoxidation of propylene and ethylene on silver and silver-gold alloy catalysts. *J. Catal.* **1982**, 77, 499–510. [CrossRef]
- 124. Mullen, G.M.; Zhang, L.; Evans, E.J.; Yan, T.; Henkelman, G.; Mullins, C.B. Oxygen and hydroxyl species induce multiple reaction pathways for the partial oxidation of allyl alcohol on gold. *J. Am. Chem. Soc.* **2014**, 136, 6489–6498. [CrossRef] [PubMed]
- 125. Mullen, G.M.; Zhang, L.; Evans, E.J.; Yan, T.; Henkelman, G.; Mullins, C.B. Control of selectivity in allylic alcohol oxidation on gold surfaces: The role of oxygen adatoms and hydroxyl species. *Phys. Chem. Chem. Phys.* **2015**, *17*, 4730–4738. [CrossRef] [PubMed]
- 126. Ojeda, M.; Iglesia, E. Catalytic epoxidation of propene with H<sub>2</sub>O-O<sub>2</sub> reactants on Au/TiO<sub>2</sub>. *Chem. Commun.* **2009**, 352–354. [CrossRef] [PubMed]
- 127. Lee, S.; Molina, L.M.; Lopez, M.J.; Alonso, J.A.; Hammer, B.; Lee, B.; Seifert, S.; Winans, R.E.; Elam, J.W.; Pellin, M.J.; Vajda, S. Selective propene epoxidation on immobilized Au<sub>6–10</sub> clusters: The effect of hydrogen and water on activity and selectivity. *Angew. Chem. Int. Ed.* **2009**, *48*, 1467–1471. [CrossRef] [PubMed]
- 128. Jiahui, H.; Tomoki, A.; Jérémy, F.; Tadahiro, F.; Takashi, T.; Masatake, H. Propene epoxidation with dioxygen catalyzed by gold clusters. *Angew. Chem. Int. Ed.* **2009**, *48*, 7862–7866.
- 129. Bongiorno, A.; Landman, U. Water-enhanced catalysis of CO oxidation on free and supported gold nanoclusters. *Phys. Rev. Lett.* **2005**, *95*, 106102. [CrossRef] [PubMed]
- 130. Chang, C.-R.; Wang, Y.-G.; Li, J. Theoretical investigations of the catalytic role of water in propene epoxidation on gold nanoclusters: A hydroperoxyl-mediated pathway. *Nano Res.* **2011**, *4*, 131–142. [CrossRef]
- 131. Chang, C.-R.; Huang, Z.-Q.; Li, J. Hydrogenation of molecular oxygen to hydroperoxyl: An alternative pathway for O<sub>2</sub> activation on nanogold catalysts. *Nano Res.* **2015**, *8*, 3737–3748. [CrossRef]
- 132. Liu, J.C.; Tang, Y.; Chang, C.R.; Wang, Y.G.; Li, J. Mechanistic insights into propene epoxidation with  $O_2$ – $H_2O$  mixture on  $Au_7/\alpha$ - $Al_2O_3$ : A hydroproxyl pathway from ab initio molecular dynamics simulations. *ACS Catal.* **2016**, *6*, 2525–2535. [CrossRef]
- 133. Joshi, A.M.; Delgass, W.N.; Thomson, K.T. Mechanistic implications of Au<sub>n</sub>/Ti-lattice proximity for propylene epoxidation. *J. Phys. Chem. C* **2007**, *111*, 7841–7844. [CrossRef]
- 134. Ajo, H.M.; Bondzie, V.A.; Campbell, C.T. Propene adsorption on gold particles on TiO<sub>2</sub>(110). *Catal. Lett.* **2002**, *78*, 359–368. [CrossRef]
- 135. Nijhuis, T.A.; Gardner, T.Q.; Weckhuysen, B.M. Modeling of kinetics and deactivation in the direct epoxidation of propene over gold–titania catalysts. *J. Catal.* **2005**, *236*, 153–163. [CrossRef]
- 136. Lee, W.S.; Lai, L.C.; Cem Akatay, M.; Stach, E.A.; Ribeiro, F.H.; Delgass, W.N. Probing the gold active sites in Au/TS-1 for gas-phase epoxidation of propylene in the presence of hydrogen and oxygen. *J. Catal.* **2012**, 296, 31–42. [CrossRef]
- 137. Haruta, M. Size- and support-dependency in the catalysis of gold. Catal. Today 1997, 36, 153–166. [CrossRef]
- 138. Nijhuis, T.A.; Visser, T.; Weckhuysen, B.M. The role of gold in gold–titania epoxidation catalysts. *Angew. Chem. Int. Ed.* **2005**, 44, 1115–1118. [CrossRef] [PubMed]
- 139. Turner, C.H.; Ji, J.; Lu, Z.; Lei, Y. Analysis of the propylene epoxidation mechanism on supported gold nanoparticles. *Chem. Eng. Sci.* **2017**, *174*, 229–237. [CrossRef]
- 140. Lu, Z.; Piernavieja-Hermida, M.; Turner, C.H.; Wu, Z.; Lei, Y. Effects of TiO<sub>2</sub> in low temperature propylene epoxidation using gold catalysts. *J. Phys. Chem. C* **2018**, 122, 1688–1698. [CrossRef]
- 141. Ji, J.; Lu, Z.; Lei, Y.; Turner, C.H. Mechanistic insights into the direct propylene epoxidation using Au nanoparticles dispersed on TiO<sub>2</sub>/SiO<sub>2</sub>. *Chem. Eng. Sci.* **2018**, *191*, 169–182. [CrossRef]
- 142. Chen, J.; Halin, S.J.A.; Schouten, J.C.; Nijhuis, T.A. Kinetic study of propylene epoxidation with H<sub>2</sub> and O<sub>2</sub> over Au/Ti-SiO<sub>2</sub> in the explosive regime. *Faraday Discuss.* **2011**, *152*, 321–336. [CrossRef] [PubMed]
- 143. Taylor, B.; Lauterbach, J.; Blau, G.E.; Delgass, W.N. Reaction kinetic analysis of the gas-phase epoxidation of propylene over Au/TS-1. *J. Catal.* **2006**, 242, 142–152. [CrossRef]

Catalysts 2018, 8, 421 24 of 24

144. Zwijnenburg, A.; Makkee, M.; Moulijn, J.A. Increasing the low propene epoxidation product yield of gold/titania-based catalysts. *Appl. Catal. A* **2004**, 270, 49–56. [CrossRef]

- 145. Green, I.X.; Tang, W.; Neurock, M.; Yates, J.T. Localized partial oxidation of acetic acid at the dual perimeter sites of the Au/TiO<sub>2</sub> catalyst—Formation of gold ketenylidene. *J. Am. Chem. Soc.* **2012**, *134*, 13569–13572. [CrossRef] [PubMed]
- 146. Green, I.X.; Tang, W.; Neurock, M.; Yates, J.T. Mechanistic insights into the partial oxidation of acetic acid by O<sub>2</sub> at the dual perimeter sites of a Au/TiO<sub>2</sub> catalyst. *Faraday Discuss.* **2013**, *162*, 247–265. [CrossRef] [PubMed]
- 147. McEntee, M.; Tang, W.; Neurock, M.; Yates, J.T. Selective catalytic oxidative-dehydrogenation of carboxylic acids—Acrylate and crotonate formation at the Au/TiO<sub>2</sub> interface. *J. Am. Chem. Soc.* **2014**, *136*, 5116–5120. [CrossRef] [PubMed]
- 148. Ntainjua, E.N.; Freakley, S.J.; Hutchings, G.J. Direct synthesis of hydrogen peroxide using ruthenium catalysts. *Top. Catal.* **2012**, *55*, 718–722. [CrossRef]
- 149. Edwards, J.K.; Freakley, S.J.; Carley, A.F.; Kiely, C.J.; Hutchings, G.J. Strategies for designing supported gold–palladium bimetallic catalysts for the direct synthesis of hydrogen peroxide. *Acc. Chem. Res.* **2014**, 47, 845–854. [CrossRef] [PubMed]
- 150. Gudarzi, D.; Ratchananusorn, W.; Turunen, I.; Heinonen, M.; Salmi, T. Promotional effects of au in Pd–Au bimetallic catalysts supported on activated carbon cloth (ACC) for direct synthesis of H<sub>2</sub>O<sub>2</sub> from H<sub>2</sub> and O<sub>2</sub>. *Catal. Today* **2015**, 248, 58–68. [CrossRef]
- 151. Yohei, N.; Tatsumi, I.; Yuiko, H.; Kotaro, K.; Kenji, K.; Hiroshige, M. Nanocolloidal Pd-Au as catalyst for the direct synthesis of hydrogen peroxide from H<sub>2</sub> and O<sub>2</sub>. *ChemSusChem* **2008**, *1*, 619–621.
- 152. Haruta, M.; Yamada, N.; Kobayashi, T.; Iijima, S. Gold catalysts prepared by coprecipitation for low-temperature oxidation of hydrogen and of carbon monoxide. *J. Catal.* **1989**, *115*, 301–309. [CrossRef]
- 153. Haruta, M. Catalysis of gold nanoparticles deposited on metal oxides. CATTECH 2002, 6, 102-115. [CrossRef]
- 154. Hashmi, A.S.; Hutchings, G.J. Gold catalysis. *Angew. Chem. Int. Ed.* **2006**, 45, 7896–7936. [CrossRef] [PubMed]



© 2018 by the authors. Licensee MDPI, Basel, Switzerland. This article is an open access article distributed under the terms and conditions of the Creative Commons Attribution (CC BY) license (http://creativecommons.org/licenses/by/4.0/).